Binding of a pathogen effector to rice Exo70 proteins tethered to the NOI/RIN4 integrated domain of the NLR receptor Pii2 confers immunity against fungi

Koki Fujisaki[1*], Yoshiko Abe[1], Yu Sugihara[2,3], Keiichiro Nemoto[1], Kazue Ito[1], Eiko Kanzaki[1], Kazuya Ishikawa[1,4], Mari Iwai[1], Hiroe Utsushi[1], Hiromasa Saitoh[1,5], Hiroki Takagi[1,6], Takumi Takeda[1], Akira Abe[1], Shuan Zheng[2], Aleksandra Bialas[3], Mark J Banfield[7], Sophien Kamoun[3] and Ryohei Terauchi[1,2*].

Affiliations

1 Iwate Biotechnology Research Center, Kitakami, Iwate, Japan.

2 Laboratory of Crop Evolution, Kyoto University, Muko, Kyoto, Japan.

3 The Sainsbury Laboratory, Norwich Research Park, Norwich, UK.

4 Ritsumeikan Global Innovation Research Organization, Ritsumeikan University, Kusatsu, Shiga, Japan.

5 Department of Molecular Microbiology, Tokyo University of Agriculture, Setagaya, Tokyo, Japan.

6 Ishikawa Prefectural University, Suematsu, Nonoichi, Ishikawa, Japan.

7 Dept. of Biochemistry and Metabolism, John Innes Centre, Norwich Research Park, Norwich, UK.

*Co-corresponding authors: Koki Fujisaki (k-fujisaki@ibrc.or.jp) and Ryohei Terauchi (terauchi@ibrc.or.jp)

ORCIDs

Koki Fujisaki: 0000-0002-8247-6381
Yu Sugihara: 0000-0001-6042-1091
Keiichiro Nemoto: 0000-0003-3540-2002
Kazuya Ishikawa: 0000-0001-7666-2906
Hiromasa Saitoh: 0000-0002-0124-9276
Hiroki Takagi: 0000-0002-8576-9892
Takumi Takeda: 0000-0003-3718-9006
Akira Abe: 0000-0002-0344-2643
Aleksandra Białas: 0000-0002-1135-2189
Mark J Banfield: 0000-0001-8921-3835
Sophien Kamoun: 0000-0002-0290-0315
Ryohei Terauchi: 0000-0002-0095-4651

Keywords: effector, plant immunity, NLR, integrated domain, rice blast.

Abstract

As much as 10% of plant immune receptors from the nucleotide-binding domain leucine-rich repeat (NLR) family carry integrated domains (IDs) that can directly bind pathogen effectors. However, it remains unclear whether direct binding to effectors is a universal feature of ID-containing NLRs given that only a few NLR-IDs have been functionally characterized. Here we show that the rice (*Oryza sativa*) sensor NLR-ID Pii2 confers resistance to strains of the rice blast fungus *Magnaporthe oryzae* that carry the effector AVR-Pii without directly binding this protein. First, we show that AVR-Pii binds the exocyst subunit OsExo70F2 in rice (*Oryza sativa*) to dissociate preformed complexes of OsExo70F2 with host RPM1 INTERACTING PROTEIN4 (RIN4) at the conserved NOI motif, facilitating a possible virulence function. Second, we show that in its resting state, Pii2 binds OsExo70F2 and OsExo70F3, essential components of *Pii*-mediated resistance, through its integrated NOI domain. Remarkably, AVR-Pii binding to OsExo70F2/F3 leads to dissociation of the Pii2–OsExo70F2 and Pii2–OsExo70F3 complexes, destabilization of Pii2, and activation of immunity. These findings support a novel conceptual model in which an NLR-ID monitors alterations of tethered host proteins targeted by pathogen effectors, providing insight into pathogen recognition mechanisms.

(193 words)

65 **Significance statement**

66 Plant diseases diminish crop yields by over 20% each year, and deploying resistant crops
67 is the most effective way to combat them. Nucleotide-binding domain leucine-rich repeat
68 (NLR)-type receptors are the major player in plant resistance against pathogens, with a
69 subset of NLRs containing unconventional domains called integrated domains (ID)
70 derived from host proteins. Previous studies suggest that pathogen avirulence (AVR)
71 effectors directly bind or modify NLR-IDs before they are recognized by the host. Here,
72 we reveal that the rice NLR-ID receptor Pii2 indirectly recognizes AVR-Pii when the
73 effector dissociates Pii2 from the host Exo70 proteins tethered to Pii2. We propose a new
74 model of how NLRs can recognize pathogens, expanding our understanding of plant
75 immunity.

76 (115 words)

77

78

Main text

Introduction

Plants have evolved immune receptors to detect and defend themselves against pathogen infections. These receptors include cytosolic nucleotide-binding domain leucine-rich repeat (NLR) proteins that recognize pathogen avirulence (AVR) effectors and activate a complex immune response including a hypersensitive response (HR) leading to localized death of infected cells. Plant NLRs have a modular architecture mostly comprising either an N-terminal coiled-coil (CC) or a Toll/interleukin-1 receptor (TIR) homology domain, followed by nucleotide-binding (NB) and leucine-rich repeat (LRR) domains. Several models have been proposed to explain how NLRs function as singletons, in pairs, or in networks [Adachi et al., 2019]. HOPZ-ACTIVATED RESISTANCE1 (ZAR1), a singleton NLR with N-terminal CC domain of *Arabidopsis* (*Arabidopsis thaliana*), forms a homo-NLR pentamer "resistosome" complex after perception of pathogen AVRs to activate immune responses [Wang et al., 2019]. Several reports have shown that NLR pairs encoded by linked genes (*RESISTANT TO P. SYRINGAE4* [*RPS4*] and RESISTANT TO RALSTONIA SOLANACEARUM1 (*RRS1*) in *Arabidopsis*, *R-GENE ANALOG4* [*RGA4*] and *RGA5* or *Pikp-1* and *Pikp-2* in rice [*Oryza sativa*]) are both required for the recognition of their cognate AVRs [Narusaka et al., 2009; Okuyama et al., 2011; Yuan et al., 2011; Cesari et al., 2014; Zdrzałek et al., 2020]. In these pairs, one NLR functions as a sensor NLR that perceives pathogen effectors, while the other NLR is a so-called helper NLR that activates immune signaling [Baggs et al., 2017; Cesari, 2018].

101 As much as 10% of all known NLRs contain additional unconventional domains
102 called integrated domains (IDs) that appear to have originated from the host targets of
103 effectors [Cesari et al., 2014; Sarris et al., 2016. The current view is that these NLRs with
104 IDs (NLR-IDs) are baits or decoys that bind pathogen effectors or serve as substrates for
105 effectors to detect invading pathogens. One example is *Arabidopsis* RRS1, an NLR that
106 carries a C-terminal domain with similarity to WRKY transcription factors. RRS1
107 perceives the bacterial effectors PopP2 from *Ralstonia solanacearum* and AvrRps4 from
108 *Pseudomonas syringae*, which normally target *Arabidopsis* WRKY proteins to enhance
109 virulence. The presence of the WRKY-like domain within RRS1 led to the proposal that
110 this domain targeted by pathogen effectors is integrated into the NLR, enabling
111 recognition of bacterial effectors [Le Roux et al., 2015; Sarris et al., 2015]. Other
112 examples include the rice NLR pairs *Pia* (RGA5 and RGA4) and *Pikp* (Pikp-1 and Pikp-
113 2), which recognize the effectors AVR-Pia/AVR1-CO39 and AVR-PikD of the rice blast
114 fungus, *Magnaporthe oryzae* (syn. *Pyricularia oryzae*), respectively [Okuyama et al.,
115 2011; Kanzaki et al., 2012; Cesari et al. 2013]. RGA5 and Pikp-1 contain a Heavy-Metal-
116 Associated (HMA) domain integrated into different positions [Okuyama et al. 2011;
117 Cesari et al., 2013; Maqbool et al., 2015]. Binding of the integrated HMA domain to the
118 corresponding AVR effectors triggers a HR and immunity against the blast fungus [Cesari
119 et al., 2013; Maqbool et al., 2015; Sugihara et al., 2023]. However, it is unclear whether
120 all NLRs with an ID recognize AVR effectors by direct ID–AVR binding. In this study,
121 we explored the diversity of ID function by analyzing the ID of the rice NLR receptor
122 Pii2, which has a unique feature of pathogen effector recognition.

123 The *Pii* locus in rice encodes a pair of CC-NLR proteins, Pii1 and Pii2, that detect
124 the *M. oryzae* effector AVR-Pii and mount an effective immune response against the
125 pathogen secreting AVR-Pii [Takagi et al., 2013 and 2017]. Despite repeated attempts
126 using various protein–protein interaction methods, we failed to detect a direct interaction
127 between AVR-Pii and Pii1 or Pii2 [Fujisaki et al., 2015]. Instead, we discovered that
128 AVR-Pii binds to two members of the large EXO70 protein family of rice, OsExo70F2
129 and OsExo70F3 [Fujisaki et al., 2015; De la Concepcion et al., 2022]; these are putative
130 subunits of the exocyst complex, an evolutionarily conserved vesicle tethering machinery
131 that functions in the last stage of exocytosis [Cvrčková et al., 2012]. Since simultaneous
132 knockdown of *OsExo70F2* and *OsExo70F3* abrogates *Pii*-mediated resistance, we
133 proposed that Pii indirectly recognizes AVR-Pii *via* host Exo70 proteins [Fujisaki et al.,
134 2015].

135 Here, we show that Pii2 recognition of AVR-Pii follows a mode of NLR perception
136 not previously described for plant pathogens: host Exo70 proteins are tethered to the
137 sensor NLR-ID Pii2, and AVR-Pii binding to Exo70F subunits causes their removal from
138 the NLR-ID, which alters Pii2 status and leads to a HR together with the helper NLR Pii1.
139

140 **Results**

141 **Rice Exo70 proteins are required for *Pii*-mediated resistance to the blast fungus**

142 Previously, we showed that simultaneous knockdown of *OsExo70F2* and *OsExo70F3*
143 genes by RNA-interference abrogated rice *Pii*-mediated resistance against *M. oryzae*
144 harboring *AVR-Pii* (Fujisaki et al. 2015). To validate this finding, we used an

145 ethylmethanesulfonate (EMS)-mediated mutant and a CRISPR/Cas9 gene knockout
146 mutant of the *Exo70* genes in the *Pii* rice background. We obtained single mutants of
147 *OsExo70F2* and *OsExo70F3* (*Osexo70f2* and *Osexo70f3*, respectively) and generated a
148 *Osexo70f2 Osexo70f3* double mutant, all in the rice cultivar Hitomebore. Single
149 knockouts of *OsExo70F2* or *OsExo70F3* did not appear to affect *Pii*-mediated resistance,
150 as evidenced by the small lesions seen when these plants were inoculated with the *M.*
151 *oryzae* strain Sasa2–AVR-Pii (Fig. 1A, 1B; Fig. S1; Vo et al., 2019). By contrast, the
152 *Osexo70f2 Osexo70f3* double knockouts showed no resistance, indicating that
153 OsExo70F2 and OsExo70F3 have redundant functions and each is sufficient for *Pii*-
154 mediated resistance (Fig. 1A, 1B and Fig. S1).
155
156 **Unlike AVR-Pii, rice Exo70 proteins bind NOI integrated-domain of Pii2**
157 We used protein interaction assays to determine the binding spectrum of Pii2. In a yeast
158 (*Saccharomyces cerevisiae*) two-hybrid (Y2H) assay, we detected an interaction between
159 OsExo70F3 and full-length Pii2 (Figs. S2 and S3A). We delineated the Exo70-interacting
160 region of Pii2 to 103 amino acids in its C terminus (Pii2-CTC for C-terminal half of Pii2-
161 specific CT region; Lee et al., 2009) (Fig. 2A; Fig. S4). In a series of Y2H assays (Fig.
162 2B, and Fig. S3C), we observed a specific interaction between Pii2-CTC and both
163 OsExo70F2 and OsExo70F3, while AVR-Pii did not interact with any regions of Pii1 or
164 Pii2 (Figs. 2B, S2, S3B, and S5). We confirmed the above interactions using an
165 AlphaScreen (Amplified Luminescent Proximity Homogenous Assay Screen), which
166 relies on the proximity of two potentially interacting proteins to emit fluorescence by

167 acceptor beads (Figs. S6, S7 and S8). Notably, the Pii2-CTC region contains a six-amino-
168 acid stretch showing similarity to the core motif of the nitrate-induced (NOI) domain
169 (PxFGxW) (Fig. 2C and Fig. S9A) [Zhao et al., 2021].
170

171 **The RIN4-like NOI motif of Pii2 is required for binding to Exo70**

172 The NOI domain is also present in *Arabidopsis* RPM1-INTERACTING PROTEIN4
173 (RIN4), which negatively regulates plant defense and is targeted by the bacterial effectors
174 AvrRpt2, AvrB, and AvrRpm1 [Kim et al., 2005]. In fact, the effector AvrRpt2 has
175 protease activity and cleaves RIN4 within its NOI motif [Chisholm et al., 2005]. To
176 investigate the possible importance of the NOI core motif of Pii2, we introduced multiple
177 mutations (Pii2-m1 variant) to replace conserved amino acid residues in this region with
178 alanines (Fig. 2D) and tested the m1 mutant for binding to OsExo70F2 and OsExo70F3.
179 In a Y2H assay and an AlphaScreen, the m1 mutant displayed compromised Pii2 binding
180 to OsExo70F2 and OsExo70F3 (Figs. 2E, S10 and S11). These results highlight the
181 importance of the Pii2 ID NOI core motif in Pii2–OsExo70F2 and Pii2–OsExo70F3
182 interactions.
183

184 **NOI domain of Pii2 has evolved from NOI-C domain of RIN4 proteins**

185 RIN4 proteins have two NOI domains, NOI-N and NOI-C, at their N and C termini,
186 respectively [Afzal et al., 2013]. A BLAST search using *Arabidopsis* RIN4 as query
187 identified six rice RIN4-like proteins (OsRIN4a–f; Fig. S12) and three rice proteins
188 containing one NOI core motif (OsNOIa–c; Fig. S13). *OsRIN4c* and *OsRIN4d* were

189 expressed in rice leaves (Fig. S14), and their protein products interacted with OsExo70F2
190 and OsExo70F3, unlike the proteins with a single NOI core motif (Fig. 2F and Fig. S15).
191 OsRIN4c showed a strong interaction with OsExo70F2 and OsExo70F3 in Y2H assays
192 (Fig. 2F) and co-immunoprecipitated from protein extracts of *Nicotiana benthamiana*
193 leaves infiltrated with *FLAG-OsRIN4c* and StrepII and HA (SH)-tagged *OsExo70F2* or
194 *OsExo70F3* constructs (Fig. S16). Importantly, mutating the C-terminal NOI (PxFGxW)
195 motif abolished these interactions (Fig. S17). The amino acid sequence of the Pii2 NOI
196 ID indicated that it is more closely related to OsRIN4 NOI-C than to NOI-N (Fig. 2G),
197 suggesting that the NOI core motif of Pii2 is most likely derived from the NOI-C of RIN4-
198 like proteins.
199
200 **NOI domain of Pii2 is required for its stability and resistance to blast fungus**
201 To explore the role of Pii2 ID in *Pii*-mediated resistance, we tested the ability of a *Pii2*
202 transgene incorporating the m1 mutation in the sequence encoding the NOI core motif
203 (Fig. 2D) to achieve transgenic rescue. We identified a *pii2* mutant rice line, Hit5882,
204 among 5,600 ethylmethanesulfonate (EMS)-mutated lines of the rice cultivar Hitomebore.
205 The mutant version of Pii2 in Hit5882 carries an amino acid substitution (V371D) in the
206 Pii2 NB-domain (Fig. S9A). When we introduced a transgene comprising the full-length
207 coding sequence of Pii2 cloned in-frame with a FLAG tag sequence (*Pii2FL2*; Fig. S9A)
208 and driven by the cauliflower mosaic virus 35S promoter into Hit5882, Pii2FL2 protein
209 was expressed and accumulated (Fig. 3A) and *Pii*-mediated resistance was restored (Fig.
210 3B, Fig. S18). By contrast, transgenic Hit5882 plants harboring a 35S:*Pii2FL2-m1*

211 transgene showed low accumulation of Pii2FL2-m1 protein (Fig. 3A) and no *Pii*-
212 mediated resistance (Fig. 3B and Fig. S18). These results suggest that the m1 mutation
213 not only abrogates Pii2 interactions with OsExo70F2 and OsExo70F3 (Fig. 2E and Fig.
214 S10) but also disrupts the stable accumulation of Pii2 *in planta*, demonstrating its serious
215 effects on *Pii*-mediated resistance.
216
217 **AVR-Pii co-expression with OsExo70F2/F3 reduces Pii2 protein accumulation**
218 We assessed the link between Pii2 binding to OsExo70F2 and OsExo70F3 and Pii2
219 accumulation *in vivo*. Accordingly, we co-transfected rice protoplasts with constructs
220 encoding Pii1, Pii2FL2, and OsExo70F2, OsExo70F3, and/or AVR-Pii in various
221 combinations. Although we did not induce a strong HR in this system (Fig. S19), we did
222 notice that co-expression of *Pii2FL2* and *OsExo70F2* or *OsExo70F3* led to enhanced
223 accumulation of Pii2FL2, an effect that was suppressed by co-expression of *AVR-Pii* but
224 not *AVR-Pii*^{Y64A} (as negative control) (Fig. 4). By contrast, we did not observe enhanced
225 accumulation of Pii2FL2-m1 when we co-expressed *Pii2FL2-m1* with *OsExo70F2* or
226 *OsExo70F3* (Fig. S20). These results suggest that NOI ID-mediated binding to Exo70 is
227 crucial for Pii function *via* stable accumulation of Pii2 in rice cells.
228
229 **AVR-Pii dissociation of the Pii2–OsExo70 complex triggers Pii2-mediated resistance**
230 To elucidate the effect of AVR-Pii on the OsExo70–OsRIN4 and OsExo70–Pii2
231 interactions, we turned to an AlphaScreen. We first examined the effect of AVR-Pii on
232 the OsExo70F2–OsRIN4c interaction. To this end, we first mixed FLAG-tagged

233 OsRIN4c and biotinylated OsExo70F2 before adding AVR-Pii to study its effect on the
234 preassembled OsRIN4c–OsExo70F2 complex (Fig. 5A). After AVR-Pii was added, the
235 AlphaScreen signal intensity decreased in a dose-dependent manner (Fig. 5B, Fig. S21).
236 This result suggests that AVR-Pii dissociates the OsRIN4c–OsExo70F2 complex,
237 possibly representing the function of AVR-Pii as an effector. We performed a similar
238 analysis using AVR-Pii and preassembled Pii2–OsExo70F2 and Pii2–OsExo70F3
239 complexes (Fig. 5A). After the addition of AVR-Pii, the AlphaScreen signal intensity
240 decreased in a dose-dependent manner (Fig. 5C, Figs. S8), mirroring the AVR-Pii effect
241 on the RIN4–OsExo70 interactions. In a series of AlphaScreens, AVR-Pii^{Y64A}, which
242 does not bind OsExo70, did not disrupt the interaction of OsExo70 with OsRIN4c or Pii2.
243 From these results, we propose that AVR-Pii manipulates plant immunity *via* altering the
244 RIN4–Exo70 interaction, and that Pii monitors this AVR-Pii action by presenting a NOI
245 ID–Exo70 interaction decoy (Fig. 6).
246
247 **Discussion**
248 The current view of plant immunity is that IDs of NLR immune receptors directly bind
249 to or serve as substrates for pathogen effectors. Our findings suggest that NLR-IDs may
250 detect host proteins targeted by pathogen effectors in a previously unrecognized
251 mechanism whereby NLR-ID mediates indirect recognition of a pathogen effector [Dangl
252 and Jones, 2001; van der Hoon and Kamoun, 2008] (Fig. 6). This model does not match
253 any of the nine mechanisms of plant disease resistance proposed previously [Kourelis and
254 van der Hoorn, 2018]. In *Arabidopsis*, RIN4 is a crucial regulator of plant immunity [Ray

255 et al., 2019]. Considering the recent reports of RIN4–EXO70 interactions [Afzal et al.,
256 2013; Sabol et al., 2017; Wu et al., 2021], we propose that rice RIN4–EXO70 complexes
257 are the target of AVR-Pii as a virulence effector (Fig. 6). We hypothesize that 1) the Pii2–
258 OsExo70F2 and Pii2–OsExo70F3 complexes are sensors and 2) the dissociation of Pii2
259 from OsExo70F2 or OsExo70F3 by AVR-Pii activates Pii2 (unstable form) to trigger
260 immune responses. (Fig. 6). Based on the previous reports, the activation of immune
261 response seems to be cooperatively executed by Pii1 and Pii2 (Takagi et al., 2013; Takagi
262 et al., 2017). Current helper / sensor model for paired NLRs suggests that Pii2 functions
263 as the sensor NLR, which may activate the helper NLR Pii1. The effects of altered Pii2
264 status on Pii1 function is the next important issue to understand the regulatory mechanism
265 of the Pii NLR system.

266 Our work also points to the NOI–EXO70 complex as a major target of plant pathogen
267 effectors. It is perhaps not surprising that these domains have been acquired as sensor
268 domains by NLR immune receptors, with NOI and EXO70 commonly seen integrated
269 into NLRs [Sarris et al., 2016; Brabham et al., 2017]. Whether integrated NOI and EXO70
270 domains can mediate the direct recognition of effectors remains to be determined.
271 Nonetheless, our finding that NLR-IDs can indirectly detect AVR effectors expands the
272 mechanistic view of pathogen detection by immune receptors: that is, the interactors of
273 NLR-IDs can be either pathogen effectors or host proteins that are targeted by effectors.
274 This work presents the first example to our knowledge of indirect pathogen recognition
275 *via* the ID of an NLR, highlighting how the arms race between plants and pathogens has
276 driven the emergence of a wealth of molecular interactions and mechanisms.

277

278 **Materials and Methods**

279

280 **Plants and pathogens**

281 *Pii2* and *OsExo70F2* knockout lines (Hit5882 and Hit3025, respectively) were isolated
282 from EMS-treated mutant lines of the rice (*Oryza sativa*) cultivar Hitomebore [Takagi et
283 al., 2013, 2017]. *OsExo70F3* knockout plants were generated using the CRISPR/Cas9
284 system with the pCRISPR/Cas9-F3-1 plasmid. *Agrobacterium tumefaciens* (EHA105)
285 was transformed with the plasmid and used for stable transformation of Hitomebore.
286 Transformation and regeneration of rice plants were performed according to Hiei et al.
287 (1994). *Osexo70f2 Osexo70f3* double knockout lines were generated by pCRISPR/Cas9-
288 F3-1-mediated knockout of *OsExo70F3* in the Hit3025 (*Osexo70f2* knockout)
289 background.

290 To generate transgenic rice plants expressing *Pii2FL1*, *Pii2FL2*, *Pii2FL3*, or *Pii2FL2-*
291 *m1*, the plasmids pCAMBIA-Pii2FL1, pCAMBIA-Pii2FL2, pCAMBIA-Pii2FL3, and
292 pCAMBIA-Pii2FL2m1, respectively, were introduced to *A. tumefaciens* EHA105, which
293 was subsequently used for transformation of Hit5882, a *pii2* mutant of the rice cultivar
294 Hitomebore [Takagi et al., 2017].

295 *Magnapothe oryzae* isolate Sasa2 is stored at Iwate Biotechnology Research Center.
296 A transgenic Sasa2 line expressing *AVR-Pii* (Sasa2-AVR-Pii) was previously established
297 as Sasa2(+22p:pex33) [Yoshida et al., 2009]. For generating transgenic Sasa2 lines
298 expressing *AVR-Pii* mutants (m9-9, Y64D, and Y64A), the plasmids pCB-pex22p-AVR-

299 Pii^{m9-9}, pCB-pex22p-AVR-Pii^{Y64D}, and pCB-pex22p-AVR-Pii^{Y64A}, respectively, were
300 used for transformation of Sasa2 following the method described by Sugihara et al. (2023).
301
302 **Generation of AVR-Pii mutants**
303 For generation of *AVR-Pii* mutants, random mutagenesis of pGAD-AVR-Pii using a
304 Diversify^{TM} PCR Random Mutagenesis Kit (Takara) was performed using primers
305 KF777f and KF778r [Fujisaki et al., 2015]. The resulting PCR products were digested
306 with *Eco*RI and *Bam*HI and introduced into pGADT7 (Clontech, CA, USA) by utilizing
307 *Eco*RI and *Bam*HI sites. pGADT7 vectors carrying *AVR-Pii* mutants including pGAD-
308 pex22p-AVR-Pii-m9-9 (AVR-Pii M4; De la Concepcion et al., 2022) were cloned and
309 used for Y2H assays in combination with pGBKT7-OsExo70F3 to verify the effects of
310 AVR-Pii mutations on the interaction with OsExo70F3 [De la Concepcion et al., 2022].
311
312 **Expression of rice genes encoding NOI core motifs**
313 The amino acid sequence of the *Arabidopsis* RIN4 protein (NP_189143.2) was used as
314 the query for a BLAST search to identify protein-coding genes containing the NOI core
315 motif (PxFGxW) in rice. To analyze gene expression, a conidial suspension (5×10^5
316 conidia/ml) of Sasa2 containing 0.002% (v/v) Tween 20 was sprayed onto Hitomebore
317 leaves and the leaves were harvested at 3 dpi. Hitomebore leaves treated with distilled
318 water with 0.002% (v/v) Tween 20 (Mock) were used as a control. Total RNA of the
319 harvested leaves was extracted using a NucleoSpin RNA Plant kit (Takara). cDNA was
320 synthesized using the ReverTra Ace kit (TOYOBO, Osaka, Japan) with oligo dT primer.

321 The primer sets used for RT-PCR of each gene are listed in Table S2. RT-PCR was
322 performed as described previously [Fujisaki et al., 2015]. The rice actin gene
323 (Os01g0866100) was amplified by RT-PCR and used as a control.
324
325 **Protein–protein interactions**
326 Y2H assays were performed as described by Kanzaki et al. [2012]. Ten-times dilution
327 series [OD_{600} = 3.0 (×1), 0.3 (×10^{-1}), and 0.03 (×10^{-2})] of yeast cells were prepared and
328 spotted onto quadruple dropout medium (QDO); basal medium lacking Trp, Leu, Ade,
329 and His but containing 5-bromo-4-chloro-3-indolyl α-D-galactopyranoside (X-α-gal)
330 (Clontech). To detect interactions, QDO medium both with and without 10 mM 3-amino-
331 1,2,4-triazole (3AT) (Sigma) was used. Yeast cells were also spotted onto double dropout
332 medium (DDO); basal medium lacking Trp and Leu to test cell viability. To determine
333 protein accumulation in yeast cells, yeast cells were propagated in liquid DDO at 30°C
334 overnight; 40 mg cells was collected by centrifugation at 15,000 × *g* for 10 sec, and
335 resuspended with 160 µl GTN + DC buffer [10% (v/v) glycerol, 25 mM Tris-HCl (pH
336 7.5), 150 mM NaCl, 1 mM DTT, and 1 tablet of protease inhibitor (Complete EDTA-
337 free ; Roche, Basel Switzerland)) before adding 160 µl of 0.6 M NaOH, mixing gently,
338 and incubating at room temperature for 10 min. Next, 160 µl of gel sample buffer [40%
339 (w/v) glycerol, 240 mM Tris-HCl (pH 6.8), 8% (w/v) SDS, 0.04% (w/v) bromophenol
340 blue, 400 mM DTT] was added and incubated at 95°C for 5 min. After centrifugation at
341 20,000 × *g* for 5 min, the supernatant was subjected to SDS-PAGE. Proteins expressed

342 from bait and prey vectors were immunologically detected using anti-Myc-tag mAb-
343 HRP-DirectT (MBL, Nagoya, Japan) and anti-HA-Peroxidase 3F10 (Roche), respectively.
344 Co-IP experiments of transiently expressed proteins in *Nicotiana benthamiana* were
345 performed as described by Fujisaki et al. [2015]. StrepII-HA (SH)-tagged OsExo70F2/F3
346 and FLAG-tagged OsRIN4c proteins were expressed using pGVG-SH-OsExo70F2,
347 pGVG-SH-OsExo70F3, and pGVG-FL-OsRIN4c, respectively. At 18 h after
348 agroinfiltration, 30 μM dexamethasone (DEX) was applied to infiltrated leaves to induce
349 transgene expression. Leaves were harvested at 24 h after DEX treatment, and their
350 homogenates in GTN buffer [Fujisaki et al., 2015] were used for co-IP. Anti-HA-Agarose
351 affinity gel (Sigma) was used for co-IP of HA-tagged proteins, and proteins were eluted
352 using 0.25 mg/ml HA peptide (Sigma).
353 For the AlphaScreen, *in vitro* transcription and protein synthesis were performed using
354 a WEPRO7240 expression kit (Cell-Free Sciences, Kanagawa, Japan) according to the
355 manufacturer's instructions. cDNA fragments were amplified from several AlphaScreen
356 plasmids carrying target genes using primers SPu and SP-A1868. *In vitro* transcripts were
357 synthesized from each cDNA fragment using SP6 RNA polymerase in a 30-μl reaction
358 mixture [6 μl of 5× transcription buffer (Cell-Free Sciences), 3 μl of 25 mM NTPs (Cell-
359 Free Sciences), 0.3 μl of SP6 RNA polymerase (80U/μl; Cell-Free Sciences), 0.3 μl of
360 RNase inhibitor (Cell-Free Sciences), 3 μl of cDNA fragment (direct use of PCR reaction
361 mixture), 17.4 μl of distilled water]. After ethanol precipitation, transcripts were
362 dissolved in 10 μl of distilled water and used for translation reactions performed in bilayer
363 mode [Takai et al., 2010] for 16 h at 16°C.

364 To detect protein–protein interactions by AlphaScreen, *in vitro* assembly of protein
365 complexes was carried out in a total volume of 15 µl containing 1 µl of biotinylated
366 proteins, and 1 µl of FLAG-tagged proteins in the AlphaScreen buffer [100 mM Tris-HCl
367 (pH 8.0), 150 mM NaCl, 0.01% (v/v) Tween 20, 1 mg/ml BSA] at 25°C for 1 h in a 384-
368 well Optiplate (PerkinElmer). For competition assays, protein complexes were first
369 assembled in a total volume of 10 µl containing 1 µl of biotinylated proteins
370 (OsExo70F2/F3) and 1 µl of FLAG-tagged protein (Pii2FL2 or FL-OsRIN4c) in the
371 AlphaScreen buffer (preformed complex). Competitor proteins (AVR-Pii and AVR-
372 Pii^{Y64A}) were diluted in a 1/5, 1/25, or 1/125 ratio with translation reaction mixture [Takai
373 et al., 2010] without mRNA, and 5 µl of competitor solution containing 1 µl of a series of
374 diluted competitor or undiluted competitor (corresponding to 0.008–1 µl of undiluted
375 competitor) was prepared in AlphaScreen buffer. After incubation of the preformed
376 complexes at 25°C for 1 h in a 384-well Optiplate, 5 µl of competitor solution was added
377 and the resulting 15 µl of protein mixture was incubated at 25°C for 1 h in a 384-well
378 Optiplate.
379 Following the instruction manual of the AlphaScreen IgG (Protein A) detection kit
380 (PerkinElmer), 10 µl of detection mixture containing AlphaScreen buffer, 5 µg/ml anti-
381 FLAG M2 antibody (Sigma-Aldrich), 0.08 µl of streptavidin-coated donor beads, and
382 0.08 µl of Protein A-coated acceptor beads were added to each well of the 384-well
383 Optiplate, followed by incubation at 25°C for 1 hr. Luminescence was measured using
384 the AlphaScreen detection program. Since OsRIN4c–OsExo70F2/F3 interactions were
385 not detected by the AlphaScreen in the presence of 150 mM NaCl, OsRIN4c-mediated

386 interactions were analyzed in the absence of NaCl. Mean values and standard deviations
387 of each complex were calculated using the signals from three wells. All results were
388 confirmed in two or more independent experiments.
389
390 **Assays for fungal pathogenicity and gene expression**
391 Rice leaf blade spot inoculation with conidial suspension (5×10^5 conidia/ml) was
392 performed as described by Sugihara et al. [2023]. Disease lesions were photographed 10–
393 12 days post-inoculation (dpi), and their vertical length was measured. To evaluate the
394 expression of transgenes in rice blast fungus carrying mutant AVR-Pii (Fig. S7), rice leaf
395 tissues (cv. Moukoto) around the disease lesions at 10 days after spot inoculation were
396 harvested, and RT-PCR was performed using primer set KF777f/KF778r. The *actin* gene
397 (MGG_03982T0) of the blast fungus was detected by RT-PCR using primers MGactinF
398 and MGactin R as a control.
399
400 **Transient gene expression in rice protoplasts**
401 Rice protoplasts were isolated from rice cell culture (Oc cell) [Ishikawa et al., 2014;
402 Ichimaru et al., 2022]. For cell wall digestion, 5 ml of packed cultured cells was mixed
403 with 25 ml of cellulase solution [4% Cellulase RS (w/v; Yakult, Tokyo, Japan), 4%
404 Cellulase R10 (w/v; Yakult), 0.1% (w/v) $CaCl_2.6H_2O$, 0.4 M mannitol, 0.1% (w/v) MES
405 pH 5.6], and incubated with gentle shaking (60 rpm) at 30°C for 3 h. After filtration
406 through Miracloth (Millipore, Billerica, MA), protoplasts in the flow-through fraction
407 were collected by centrifugation at 800 × *g*, washed two times with 20 ml of W5 buffer

408 (154 mM NaCl, 125 mM $CaCl_2$, 5mM KCl, and 2mM MES pH 5.7), and adjusted to the
409 desired concentration (2–3 × 10^6 protoplasts/ml) with W5 buffer. For transfection, 10 µl
410 of plasmid DNA containing 20 µg of the indicated combination of expression vectors
411 (e.g., 4 µg of pAHC-FL-Pii1, 8 µg of pAHC-Pii2FL2, 2 µg of pAHC-OsExo70F2, 2 µg
412 of pAHC-OsExo70F3, 2 µg of pAHC-AVR-Pii, and 2 µg of pAHC-luciferase) was mixed
413 with 100 µl of protoplast solution. Next, 110 µl of PEG solution [40% PEG4000 (w/v;
414 Fluka), 0.2 M mannitol, 0.1 M $CaCl_2$] was added to the protoplast solution, mixed gently,
415 and incubated at room temperature for 20 min. W5 buffer (700 µl) was then added, and
416 protoplasts were collected by centrifugation at 800 × *g*. The protoplasts were washed with
417 700 µl of W5 buffer, resuspended in 500 µl of W5 buffer, and incubated in the dark at
418 30°C for 20 h. After incubation, protoplasts were collected by centrifugation at 800 × *g*,
419 resuspended with 60 µl of 1 × GSB [62.5 mM Tris-HCl (pH6.8), 10% (v/v) glycerol, 0.2
420 g/ml SDS, 5µg/ml bromophenol blue, and 100 mM DTT], and subjected to
421 immunoblotting. For cell death assays, the collected protoplasts were assayed using a
422 Luciferase assay system (Promega, Madison, WI) according to the manufacturer's
423 instructions.
424
425 **Protein detection**
426 Proteins were immunologically detected by immunoblot analysis. For detection of AVR-
427 Pii protein without epitope tag, an anti-AVR-Pii antibody was produced using
428 recombinant His-AVR-Pii-ns [Fujisaki et al., 2015] as antigen. Preparation of rabbit
429 AVR-Pii-specific antiserum was performed by Scrum Inc. (Tokyo, Japan). OsExo70F2-

430 and OsExo70F3-specific antisera [Fujisaki et al., 2015], respectively, were used to detect
431 OsExo70F2 and OsExo70F3 without epitope tag expressed in rice protoplasts. Antibodies
432 bound to the antigens were detected by HRP-conjugated anti-rabbit IgG (H+L) (Promega).
433 HRP-conjugated anti-FLAG M2 (Sigma-Aldrich, St. Louis, MO), anti-HA 3F10 (Roche,
434 Basel, Switzerland), and anti-Myc-tag mAb-HRP-DirectT (MBL, Tokyo, Japan) were
435 used for the detection of FLAG-, SH-, and Myc-tagged proteins, respectively.
436 Biotinylated proteins were detected using HRP-conjugated streptavidin (Cell Signaling,
437 Danvers, MA).
438
439 **Phylogenetic analysis and BLAST search analysis**
440 hmmsearch (https://www.ebi.ac.uk/Tools/hmmer/search/hmmsearch) was used against
441 the "Reference Proteomes" for Poaceae (taxid: 4479) to search for NOI domain sequences.
442 The profile HMM PF05627, known as the NOI domain and associated with the cleavage
443 site for pathogenic type III effector avirulence factor Avr [Afzal et al., 2013], was used
444 as the query profile. The following cut-offs were applied in the hmmsearch: -T 3 --domT
445 3 --incT 5 --incdomT 5. After obtaining the sequences containing NOI domains, those
446 having any missing residues ('X') or more than two NOI domains were filtered out. The
447 six validated rice NOI protein sequences were added to the 607 retained sequences, and
448 the command-line hmmsearch v3.3.2 was executed again with the same cut-offs to
449 generate a multiple sequence alignment of NOI domains in Stockholm format. This
450 alignment was converted to FASTA format using esl-reformat. Sequences containing
451 NOI motifs without any gaps ('-') were retained for phylogenetic analysis. IQ-TREE

452 v2.2.0.3 [Minh et al., 2020; http://www.iqtree.org] with 1,000 ultrafast bootstrap
453 replicates [Hoang et al., 2018] was used for phylogenetic analysis. The best-fit model to
454 reconstruct the tree was automatically selected by ModelFinder [Kalyaanamoorthy et al.,
455 2017] in IQ-TREE, which selected "Q.plant+I+G4" according to the Bayesian
456 Information Criterion (BIC). Finally, NLR proteins were annotated using NLRtracker
457 [Kourelis et al., 2021], and the resulting phylogenetic tree was visualized and annotated
458 using iTOL [Letunic & Bork, 2021; https://itol.embl.de].

Acknowledgements and funding sources

We thank Dr. John J.A. Dominguez, Dr. Hiroyuki Kanzaki, and Sayaka Fujisaki for technical and general assistance. This work was supported by JSPS Grants 15H05779, 20H05681, 23K20042 and 24H00010 to RT and 26850029 to KF. Biotechnology and Biological Sciences Research Council (BBSRC, UK) grants BB/X010996/1 to MJB and SK and V015508/1 to MJB.

Footnotes

The authors declare no competing interests.

Data, Materials, and Methods

All data presented in this study are included in the article and/or the *SI Appendix*. The datasets used for phylogenetic analysis were uploaded to Github (https://github.com/YuSugihara/NOI_domains) and Zenodo (https://doi.org/10.5281/zenodo.11216127). Detailed information on the construction of plasmids used in this study is provided in Supplementary text S1 and Table S1, and the primer sequences used for the experiments are listed in Table S2.

479 **References**

480 1. Adachi, H., Derevnina, L., and Kamoun, S. (2019). NLR singletons, pairs and
481 networks: evolution, assembly, and regulation of the intracellular immunoreceptor
482 circuitry of plants. Curr. Opin. Plant Biol. 50, 121-131.

483 2. Wang, J., Hu, M., Wang, J., Qi, J., Han, Z., Wang, G., Qi, Y., Wang, H.W., Zhou,
484 J.M., and Chai, J. (2019). Reconstitution and structure of a plant NLR resistosome
485 conferring immunity. Science. 5, 364.

486 3. Narusaka, M., Kubo, Y., Shiraishi, T., Iwabuchi, M., and Narusaka, Y. (2009). A dual
487 resistance gene system prevents infection by three distinct pathogens. Plant Signal
488 Bihav. 4, 954-955.

489 4. Okuyama, Y., Kanzaki, H., Abe, A., Yoshida, K., Tamiru, M., Saitoh, H., Fujibe, T.,
490 Matsumura, H., Shenton, M., Galam, D.C., Undan, J., Ito, A., Sone, T., and Terauchi,
491 R. (2011). A multifaceted genomics approach allows the isolation of the rice Pia-blast
492 resistance gene consisting of two adjacent NBS-LRR protein genes. Plant J. 66, 467-
493 479.

494 5. Yuan, B., Zhai, C., Wang, W., Zeng, X., Xu, X., Hu, H., Lin, F., Wang, L., and Pan,
495 Q. (2011). The Pik-p resistance to Magnaporthe oryzae in rice is mediated by a pair
496 of closely linked CC-NBS-LRR genes. Theor. Appl. Genet. 122, 1017-1028.

497 6. Césari, S., Kanzaki, H., Fujiwara, T., Bernoux, M., Chalvon, V., Kawano, Y.,
498 Shimamoto, K., Dodds, P., Terauchi, R., and Kroj, T. (2014). The NB-LRR proteins

499 RGA4 and RGA5 interact functionally and physically to confer disease resistance.
500 EMBO J. 33, 1941-1959.
501 7. Zdrzałek, R., Kamoun, S., Terauchi, R., Saitoh, H., and Banfield, M.J. (2020). The
502 rice NLR pair Pikp-1/Pikp-2 initiates cell death through receptor cooperation rather
503 than negative regulation. PLoS one. 15, e0238616.
504 8. Baggs, E., Dagdas, G., and Krasileva, KV. (2017). NLR diversity, helpers and
505 integrated domains: making sense of the NLR IDentity. Curr. Opin. Plant Biol. 38,
506 59-67.
507 9. Cesari, S. (2018). Multiple strategies for pathogen perception by plant immune
508 receptors. New Phytol. 219, 17-14
509 10. Cesari, S., Bernoux, M., Moncuquet, P., Kroj, T., and Dodds, P.N. (2014). A novel
510 conserved mechanism for plant NLR protein pairs: the "integrated decoy" hypothesis.
511 Front Plant Sci. 5, 606.
512 11. Wu, C.H., Krasileva, K, V., Banfield, M. J., Terauchi, R., and Kamoun, S. (2015). The
513 "sensor domains" of plant NLR proteins: more than decoys. Front Plant Sci. 6,134.
514 12. Le Roux, C., Huet, G., Jauneau, A., Camborde, L., Trémousaygue, D., Kraut, A., Zhou,
515 B., Levaillant, M., Adachi, H., Yoshioka, H., Raffaele, S., Berthomé, R., Couté, Y.,
516 Parker, J.E., and Deslandes, L. (2015). A receptor pair with an integrated decoy
517 converts pathogen disabling of transcription factors to immunity. Cell. 161, 1074-
518 1088.
519 13. Sarris, P.F., Duxbury, Z., Huh, S.U., Ma, Y., Segonzac, C., Sklenar, J., Derbyshire, P.,
520 Cevik, V., Rallapalli, G., Saucet, S.B., Wirthmueller, L., Menke, F.L., Sohn, K.H., and

521 Jones, J.D. (2015). A Plant Immune Receptor Detects Pathogen Effectors that Target
522 WRKY Transcription Factors. Cell. 161, 1089-1100.
523 14. Kanzaki, H., Yoshid,a K., Saitoh, H., Fujisaki, K., Hirabuchi, A., Alaux, L., Fournier,
524 E., Tharreau, D., and Terauchi, R. (2012). Arms race co-evolution of Magnaporthe
525 oryzae AVR-Pik and rice Pik genes driven by their physical interactions. Plant J. 72,
526 894-907.
527 15. Cesari, S., Thilliez, G., Ribot, C., Chalvon, V., Michel, C., Jauneau, A., Rivas, S.,
528 Alaux, L., Kanzaki, H., Okuyama, Y., Morel, J.B., Fournier, E., Tharreau, D., Terauchi,
529 R., and Kroj, T. (2013). The rice resistance protein pair RGA4/RGA5 recognizes the
530 Magnaporthe oryzae effectors AVR-Pia and AVR1-CO39 by direct binding. Plant Cell
531 25, 1463-1481.
532 16. Maqbool, A., Saitoh, H., Franceschetti, M., Stevenson, C.E., Uemura, A., Kanzaki,
533 H., Kamoun, S., Terauchi, R., and Banfield, M.J. (2015). Structural basis of pathogen
534 recognition by an integrated HMA domain in a plant NLR immune receptor. Elife. 25,
535 4.
536 17. Sugihara, Y., Abe, Y., Takagi, H., Abe, A., Shimizu, M., Ito, K., Kanzaki, E., Oikawa,
537 K., Kourelis, J., Langner, T., Win, J., Białas, A., Lüdke, D., Contreras, M.P., Chuma,
538 I., Saitoh, H., Kobayashi, M., Zheng, S., Tosa, Y., Banfield, M.J., Kamoun, S.,
539 Terauchi, R., and Fujisaki, K. (2023). Disentangling the complex gene interaction
540 networks between rice and the blast fungus identifies a new pathogen effector. PLoS
541 Biol. 21, e30001945.
542 18. Takagi, H., Uemura, A., Yaegashi, H., Tamiru, M., Abe, A., Mitsuoka, C., Utsushi, H.,

543 Natsume, S., Kanzaki, H., Matsumura, H., Saitoh, H., Yoshida, K., Cano, L.M.,
544 Kamoun, S., and Terauchi, R. (2013). MutMap-Gap: whole-genome resequencing of
545 mutant F2 progeny bulk combined with de novo assembly of gap regions identifies
546 the rice blast resistance gene Pii. New Phytol. 200, 276-283
547 19. Takagi, H., Abe, A., Uemura, A., Oikawa, K., Utsushi, H., Yaegashi, H., Shimizu, M.,
548 Abe, Y., Kanzaki, H., Saitoh, H., Terauchi, R., and Fujisaki, K. (2017). Rice blast
549 resistance gene Pii is controlled by a pair of NBS-LRR genes Pii-1 and Pii-2. bioRXiv
550 doi. https://doi.org/10.1101/227132.
551 20. Fujisaki, K., Abe, Y., Ito, A., Saitoh, H., Yoshida, K., Kanzaki, H., Kanzaki, E.,
552 Utsushi, H., Yamashita, T., Kamoun, S., and Terauchi, R. (2015). Rice Exo70 interacts
553 with a fungal effector, AVR-Pii, and is required for AVR-Pii-triggered immunity. Plant
554 J. 83, 875-887.
555 21. De la Concepcion J.C., Fujisaki, K., Bentham, A.R., Cruz Mireles, N., Sanchez de
556 Medina Hernandez, V., Shimizu, M., Lawson, D.M., Kamoun, S., Terauchi, R., and
557 Banfield, M.J. (2022). A blast fungus zinc-finger fold effector binds to a hydrophobic
558 pocket in host Exo70 proteins to modulate immune recognition in rice. Proc. Natl.
559 Acad. Sci. USA. 119, e2210559119.
560 22. Cvrčková, F., Grunt, M., Bezvoda, R., Hála, M., Kulich, I., Rawat, A. and Zárský, V.
561 (2012). Evolution of the land plant exocyst complexes. Front Plant Sci. 3, 159.
562 23. Vo, KTX., Lee, SK., Halane, MK., Song, MY., Hoang, TV., Kim, CY., Park, SY., Jeon,
563 J., Kim, ST., Sohn, KH., and Jeon, JS. (2019). Pi5 and Pii paired NLRs are
564 functionally exchangeable and confer similar disease resistance specificity. Mol Cells.

565 42, 637-645.

566 24. Lee, S.K., Song, M.Y., Seo, Y.S., Kim, H.K., Ko, S., Cao, P.J., Suh, J.P., Yi, G., Roh,
567 J.H., Lee, S., An, G., Hahn, T.R., Wang, G.L., Ronald, P., and Jeon, J.S. (2009). Rice
568 Pi5-mediated resistance to Magnaporthe oryzae requires the presence of two coiled-
569 coil-nucleotide-binding-leucine-rich repeat genes. Genetics. 181, 1627–1638.

570 25. Zhao, G., Guo, D., Wang, L., Li, H., Wang, C., and Guo, X. (2021). Functions of
571 RPM1-interacting protein 4 in plant immunity. Planta. 253, 11.

572 26. Kim, M.G., da Cunha, L., McFall, A.J., Belkhadir, Y., DebRoy, S., Dangl, J.L., and
573 Mackey, D. (2005). Two Pseudomonas syringae type III effectors inhibit RIN4-
574 regulated basal defense in Arabidopsis. Cell. 121, 749-759.

575 27. Chisholm, ST., Dahlbeck, D., Krishnamurthy, N., Day, B., Sjolander, K., and
576 Staskawicz, BJ. (2005). Molecular characterization of proteolytic cleavage sites of
577 the Pseudomonas syringae effector AvrRpt2. Proc. Natl. Acad. Sci. USA 102, 2087-
578 2092.

579 28. Afzal,, A.J., Kim, J.H., and Mackey, D. (2013). The role of NOI-domain containing
580 proteins in plant immune signaling. BMC Genomics. 14, 327.

581 29. Dangl, J.L., and Jones, J.D. (2001). Plant pathogens and integrated defence responses
582 to infection. Nature. 411, 826-833.

583 30. van der Hoorn, R.A., and Kamoun, S. (2008). From Guard to Decoy: a new model for
584 perception of plant pathogen effectors. Plant Cell. 20, 2009-2017.

585 31. Kourelis, J., and van der Hoorn, R. (2018). Defended to the Nines: 25 years of
586 Resistance Gene Cloning Identifies Nine Mechanisms for R Protein Function. Plant

587 Cell. 30, 285-299.

588 32. Ray, SK., Macoy, DM., Kim, WY., Lee, SY., and Kim, MG. (2019). Role of RIN4 in
589 Regulating PAMP-Triggered Immunity and Effector-Triggered Immunity: Current
590 Status and Future Perspectives Mol Cells. 42, 503-511.

591 33. Sabol, P., Kullich, I., and Zarsky, V. (2017). RIN4 recruits the exocyst subunit
592 EXO70B1 to the plasma membrane. J. Exp. Bot. 68, 3253-3265.

593 34. Wu, X., Huang, J., Cao, Y., and Gao, Z. (2021). The resistance associated protein
594 RIN4 promotes the extracellular transport of AtExo70E2. Biochem Biophys Res
595 Commun. 68, 3253-3265.

596 35. Sarris, P.F., Cevik, V., Dagdas, G., Jones, J.D.G., And Krasileva, K.V. (2016).
597 Comparative analysis of plant immune receptor architectures uncovers host proteins
598 likely targeted by pathogens. BMC Biol. 14, 8.

599 36. Brabham, H.J., Hernández-Pinzón I., Hoden, S., Lorang, J., and Moscou, M.J. (2017).
600 An ancestral integration at Mla is maintained as a trans-species polymorphism.
601 BioRxiv doi. https://doi.org/10.1101/239541

602 37. Wheeler, T.J., Clements, J., and Finn, R.D. (2014). Skylign: a tool for creating
603 informative, interactive logos representing sequence alignments and profile hidden
604 Markov models. BMC Bioinformatics. 15:7.

605 38. Kourelis, J., Sakai, T., Adachi, H., and Kamoun, S. (2021). RefPlantNLR is a
606 comprehensive collection of experimentally validated plant disease resistance
607 proteins from the NLR family. PLoS Biol. 19:e3001124.

608 39. Sharma, S., Sharma, S., Hirabuchi, A., Yoshida, K., Fujisaki, K., Ito, A., Uemura, A.,
609 Terauchi, R., Kamoun, S., Sohn, K.H., Jones, J.D., and Saitoh, H. (2013). Deployment
610 of the Burkholderia glumae type III secretion system as an efficient tool for
611 translocating pathogen effectors to monocot cells. Plant J. 74; 701-712
612 40. Takai, K., Sawasaki, T., and Endo Y. (2010). Practical cell-free protein synthesis
613 system using purified embryos.Nat. Protoc. 5:227-238.
614 41. Ishikawa, K., Yamaguchi, K., Sakamoto, K., Yoshimura, S., Inoue, K., Kojima, C.,
615 and Kawasaki, T. (2014). Bacterial effector modulation of host E3 ligase activity
616 suppreses PAMP-triggered immunity in rice. Nat. Commun. 5:5430
617 42. Ichimaru, K., Yamaguchi, K., Harada, K., NIshio, Y., Ishikawa, K., Inoue, H., Shigeta,
618 S., Inoue, K., Shimada, K., Yoshimura, S., Takeda, T., Yamashita, E., Fujiwara, T.,
619 Nakagawa, A., Kojima, C., and Kawasaki, T. (2022). Cooperative regulation of PBI1
620 and MAPKs controls WRKY45 transcription factor in rice immunity. Nat. Commun.
621 13:2397.
622 43. Afzal, A. J., Kim, J. H., & Mackey, D. (2013). The role of NOI-domain containing
623 proteins in plant immune signaling. BMC Genomics, 14, 327.
624 44. Minh, B. Q., Schmidt, H. A., Chernomor, O., Schrempf, D., Woodhams, M. D., von
625 Haeseler, A., & Lanfear, R. (2020). IQ-TREE 2: New Models and Efficient Methods
626 for Phylogenetic Inference in the Genomic Era. Molecular Biology and Evolution,
627 37(5), 1530–1534.

628 45. Hoang, D. T., Chernomor, O., von Haeseler, A., Minh, B. Q., & Vinh, L. S. (2018).
629 UFBoot2: Improving the Ultrafast Bootstrap Approximation. Molecular Biology and
630 Evolution, 35(2), 518–522.
631 46. Kalyaanamoorthy, S., Minh, B. Q., Wong, T. K. F., von Haeseler, A., & Jermiin, L.
632 S. (2017). ModelFinder: Fast model selection for accurate phylogenetic estimates.
633 Nature Methods, 14(6), 587–589.
634 47. Kourelis, J., Sakai, T., Adachi, H., & Kamoun, S. (2021). RefPlantNLR is a
635 comprehensive collection of experimentally validated plant disease resistance
636 proteins from the NLR family. PLOS Biology, 19(10), e3001124.
637 48. Letunic, I., & Bork, P. (2021). Interactive Tree Of Life (iTOL) v5: An online tool for
638 phylogenetic tree display and annotation. Nucleic Acids Research, 49(W1),
639
640

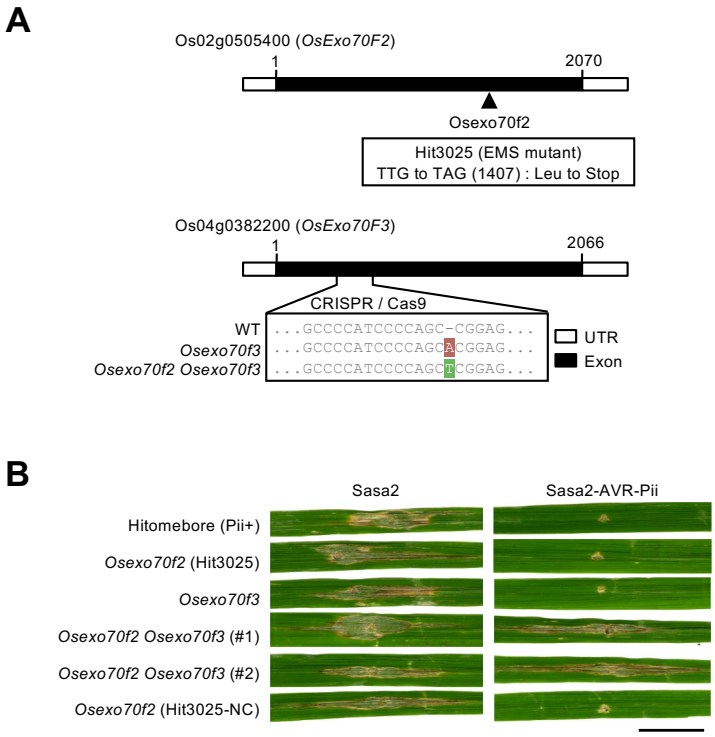

Fig. 1. The host *Exo70* genes *OsExo70F2* and *OsExo70F3* are redundantly required in *Pii*-mediated recognition of *AVR-Pii*.

(A) Isolation of single and double knockout mutants of *OsExo70F2* and *OsExo70F3*. Hit3025 is a loss-of-function mutant of *OsExo70F2* (*Osexo70f2*) in the rice cultivar Hitomebore (*Pii*+) generated by EMS mutagenesis; *Osexo70f3* is a single knockout mutant of *OsExo70F3* in Hitomebore generated by CRISPR/Cas9-mediated gene editing; *Osexo70f2 Osexo70f3* is a double knockout mutants of *OsExo70F2* and *OsExo70F3* generated by CRISPR/Cas9-mediated gene editing in the Hit3025 background.

(B) Effects of *Osexo70f2* and *Osexo70f3* single and double mutations on *Pii*-mediated resistance. Hitomebore and the single and double mutants were inoculated with the rice blast fungus isolate Sasa2 (without *AVR-Pii*) or the transgenic strain Sasa2–AVR-Pii with *AVR-Pii* [Yoshida et al., 2009]. Representative disease lesions on leaves are shown. A transgenic line (Hit3025-NC), which was derived from the same genetic transformation round as *Osexo70f2 Osexo70f3* but with no induced mutation, was used as a negative control. Knockout of *OsExo70F2* and/or *OsExo70F3* is indicated in the left.

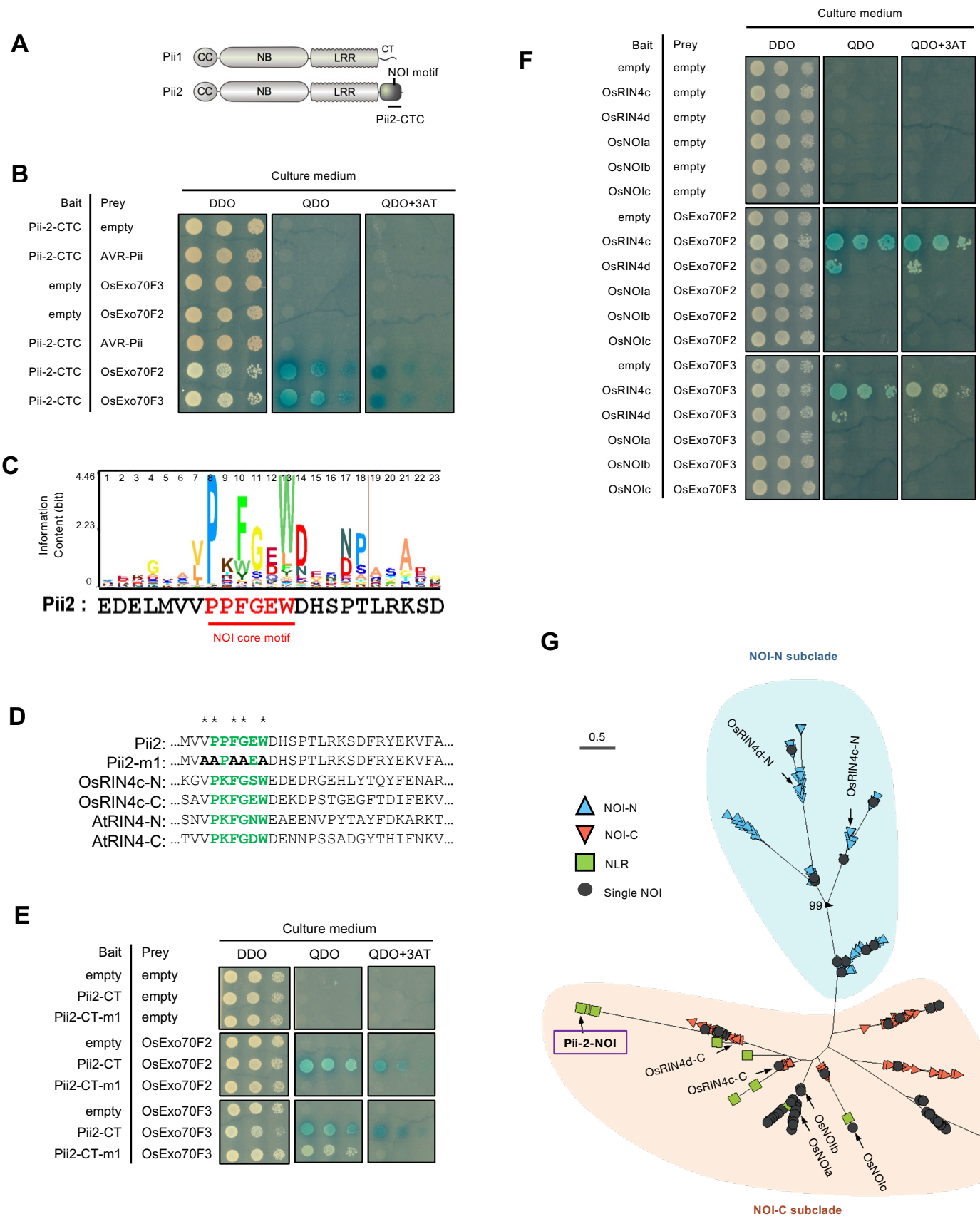
A
Pii1
CC
NB
LRR
CT
NOI motif
Pii2
CC
NB
LRR
Pii2-CTC
B
Culture medium
Bait
Prey
DDO
QDO
QDO+3AT
Pii-2-CTC empty
Pii-2-CTC AVR-Pii
empty OsExo70F3
empty OsExo70F2
Pii-2-CTC AVR-Pii
Pii-2-CTC OsExo70F2
Pii-2-CTC OsExo70F3
C
Information Content (bit)
4.46
2.23
0
Pii2 : EDELMVVPPFGEWDHSPTLRKSD
NOI core motif
D
** ** *
Pii2: ...MVVPPFGEWDHSPTLRKSDFRYEKVFA...
Pii2-m1: ...MVAAPAAEADHSPTLRKSDFRYEKVFA...
OsRIN4c-N: ...KGVPKFGSWEDEDRGEHLYTQYFENAR...
OsRIN4c-C: ...SAVPKFGEWDEKDPSTGEGFTDIFEKV...
AtRIN4-N: ...SNVPKFGNWEAEENVPYTAYFDKARKT...
AtRIN4-C: ...TVVPKFGDWDENNPSSADGYTHIFNKV...
E
Culture medium
Bait
Prey
DDO
QDO
QDO+3AT
empty empty
Pii2-CT empty
Pii2-CT-m1 empty
empty OsExo70F2
Pii2-CT OsExo70F2
Pii2-CT-m1 OsExo70F2
empty OsExo70F3
Pii2-CT OsExo70F3
Pii2-CT-m1 OsExo70F3
F
Culture medium
Bait
Prey
DDO
QDO
QDO+3AT
empty empty
OsRIN4c empty
OsRIN4d empty
OsNOIa empty
OsNOIb empty
OsNOIc empty
empty OsExo70F2
OsRIN4c OsExo70F2
OsRIN4d OsExo70F2
OsNOIa OsExo70F2
OsNOIb OsExo70F2
OsNOIc OsExo70F2
empty OsExo70F3
OsRIN4c OsExo70F3
OsRIN4d OsExo70F3
OsNOIa OsExo70F3
OsNOIb OsExo70F3
OsNOIc OsExo70F3
G
NOI-N subclade
0.5
NOI-N
NOI-C
NLR
Single NOI
OsRIN4d-N
OsRIN4c-N
99
Pii-2-NOI
OsRIN4d-C
OsRIN4c-C
OsNOIb
OsNOIa
OsNOIc
NOI-C subclade

Fig. 2 The host Exo70 proteins OsExo70F2 and OsExo70F3, but not the fungal effector AVR-Pii, interact with the NOI–integrated domain (ID) of Pii2, presumably derived from a *RIN4*-like gene.

(A) Diagram of Pii1 and Pii2 showing the Pii2 C-terminal fragment (Pii2-CTC) that binds to OsExo70F2 and OsExo70F3. The position of the NOI core motif (PxFGxW) is indicated.
(B) Yeast two-hybrid (Y2H) assay testing the interaction of Pii2-CTC with OsExo70F2, OsExo70F3, and AVR-Pii. Ten-fold serial dilution of positive yeast transformants were spotted onto double dropout (DDO) medium as control and on quadruple dropout (QDO) medium and QDO medium + 10 mM 3-amino-1,2,4-triazole (3AT) to test interactions. Empty vector (empty) was used as negative control. For additional data of mapping the interacting regions, see Figs. S2 to S5.
(C) Protein logo of the PF05627 domain generated by Skylign (Wheeler et al., 2014). Only the region around the NOI core motif (PxFGxW) is shown. The corresponding amino acid sequence from Pii2 is indicated below.
(D) Amino acid sequence alignment of NOI and surrounding sequence in Pii2, the N- and C-terminal regions of rice RIN4c (OsRIN4c-N and OsRIN4c-C) and those of Arabidopsis RIN4 (AtRIN4-N and AtRIN4-C). The conserved amino acid residues are marked by asterisks. The positions of the mutations in the Pii2-m1 mutant are indicated in bold black text.
(E) Interaction test between the Pii2-m1 mutant and OsExo70F2 or OsExo70F3 in Y2H.
(F) Y2H assay testing the interaction of rice proteins containing a NOI core motif with OsExo70F2 and OsExo70F3.
(G) Phylogenetic tree of 737 NOI domains from *Poaceae* species, using only the regions detected as NOI domains using HMMSearch. The phylogenetic tree was reconstructed by the maximum likelihood method using IQ-TREE with 1,000 bootstrap replicates. NLRs were annotated using NLRtracker (Kourelis et al., 2021). When a non-NLR protein contained two NOI domains, the N-terminal and C-terminal NOI domains were labeled as N or C. When a non-NLR protein contained a single NOI domain, the NOI domain was labeled as NOI.

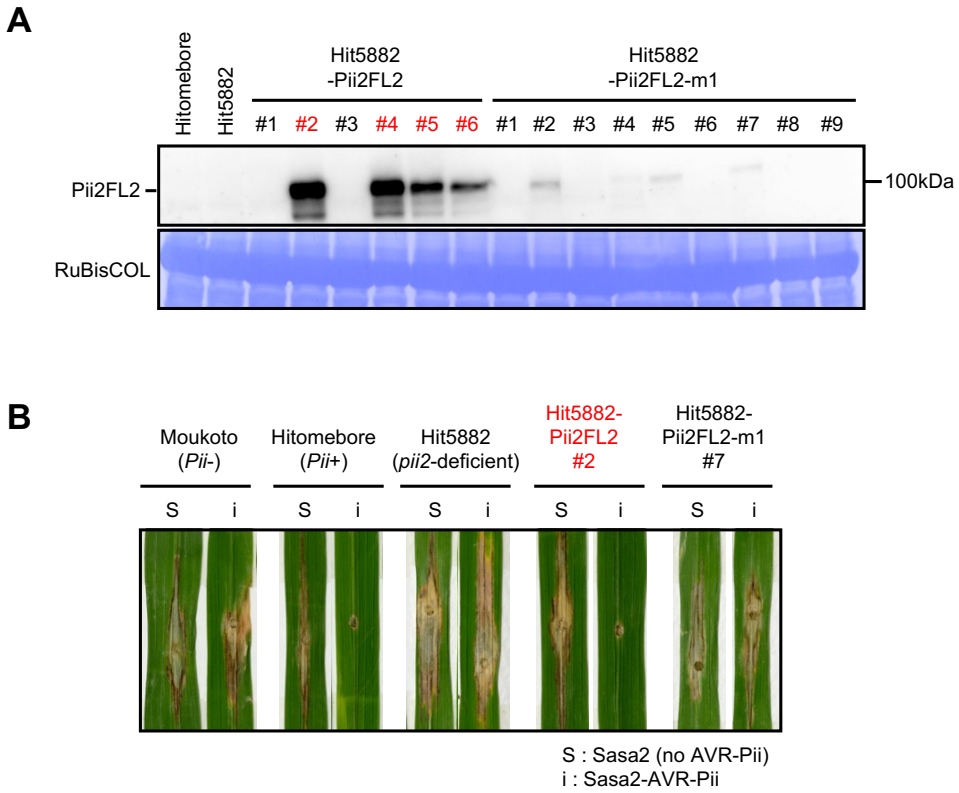

Fig. 3 The Pii2 variant carrying the m1 mutation has a low abundance in rice leaves and does not induce resistance against AVR-Pii.

(A) Pii2FL2 accumulation in transgenic rice leaves. Pii2FL2 and its m1 variant (Pii2FL2-m1) were detected by immunoblot analysis using anti-FLAG antibodies. CBB-stained RuBisCOL (Rubisco large subunit) are shown below as loading control. (B) Complementation assay by Pii2FL2 or Pii2FL2-m1. Representative data of disease lesions following inoculation of the rice cultivars Moukoto (*Pii*−), Hitomebore (*Pii*+), Hit5882 (a *pii2* mutant in Hitomebore), and Hit5882 transgenic lines expressing Pii2FL2 or Pii2FL2-m1 (Hit5882-Pii2FL2 and Hit5882-Pii2FL2-m1, respectively) with the rice blast fungus strains Sasa2 (S) and Sasa2–AVR-Pii (i). In (A–B), the transgenic lines showing *Pii*-mediated resistance are marked by red letters.

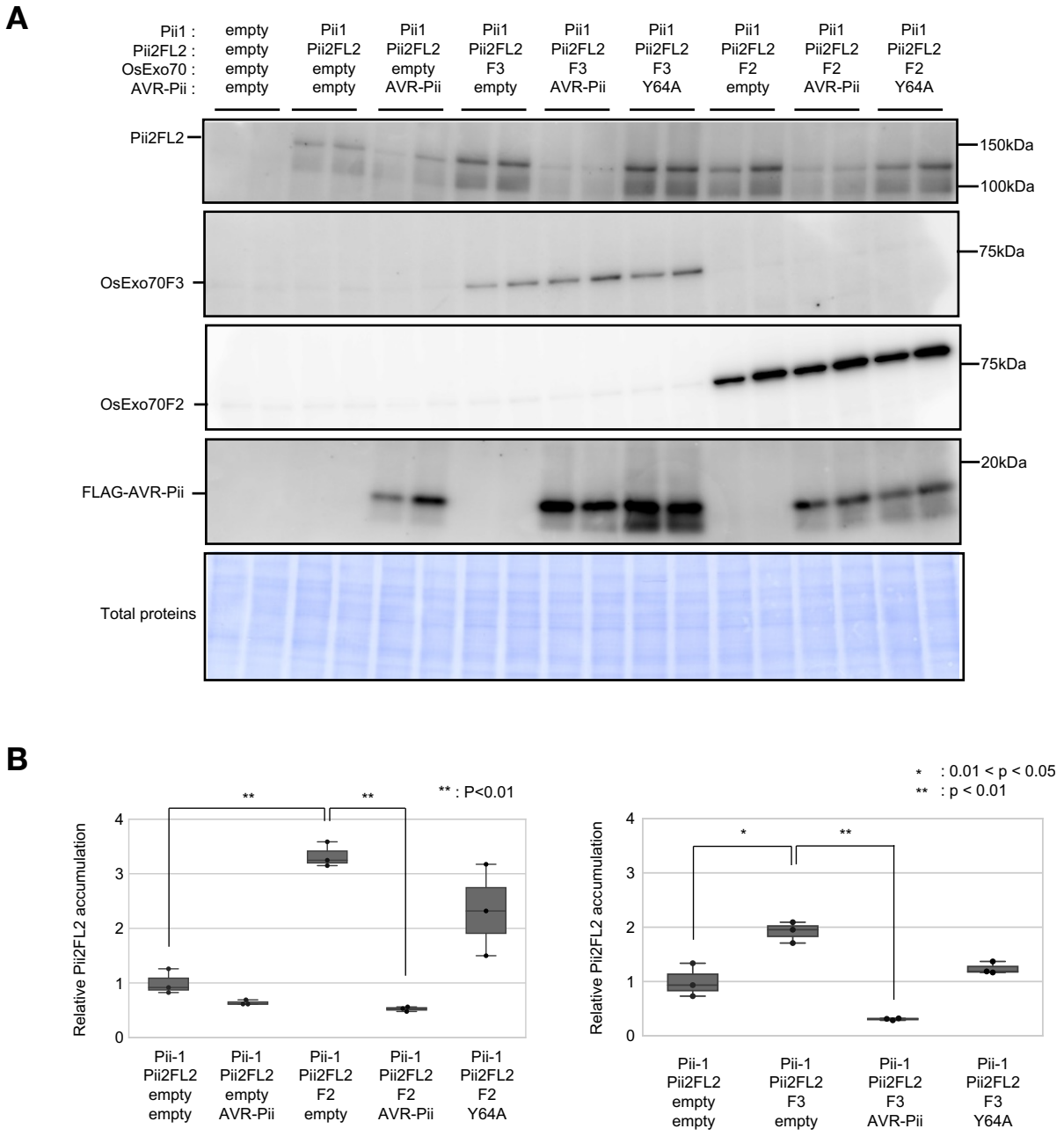

Fig. 4. Effects of co-expression of OsExo70F2/F3 and AVR-Pii on Pii2FL2 accumulation. (A) Representative data of the accumulation of the indicated proteins in the transfected protoplasts prepared from rice Oc cell culture. AVR-Pii^{Y64A} (labeled Y64A: a loss-of-function mutant of AVR-Pii; see Fig. S7) was used as negative control. Pii2FL2 and FLAG-AVR-Pii were detected by immunoblot analysis using anti-FLAG antibodies. OsExo70F2 and OsExo70F3 were detected using a specific antiserum. The combinations of transfected constructs are indicated above. (B) Quantification of the abundance of Pii2FL2 encoded by the *Pii2FL2* construct, co-expressed with *AVR-Pii*, *AVR-Pii^{Y64A}*, *OsExo70F2* (left), and/or *OsExo70F3* (right). Protein band intensity was quantified using ImageJ (https://imagej.net/ij/). Boxplots were illustrated from the values of three technical replicates. Single (*t*-test; $0.01<P<0.05$) and double (*t*-test; $P<0.01$) asterisks represent significant differences of Pii2FL2 accumulation levels.

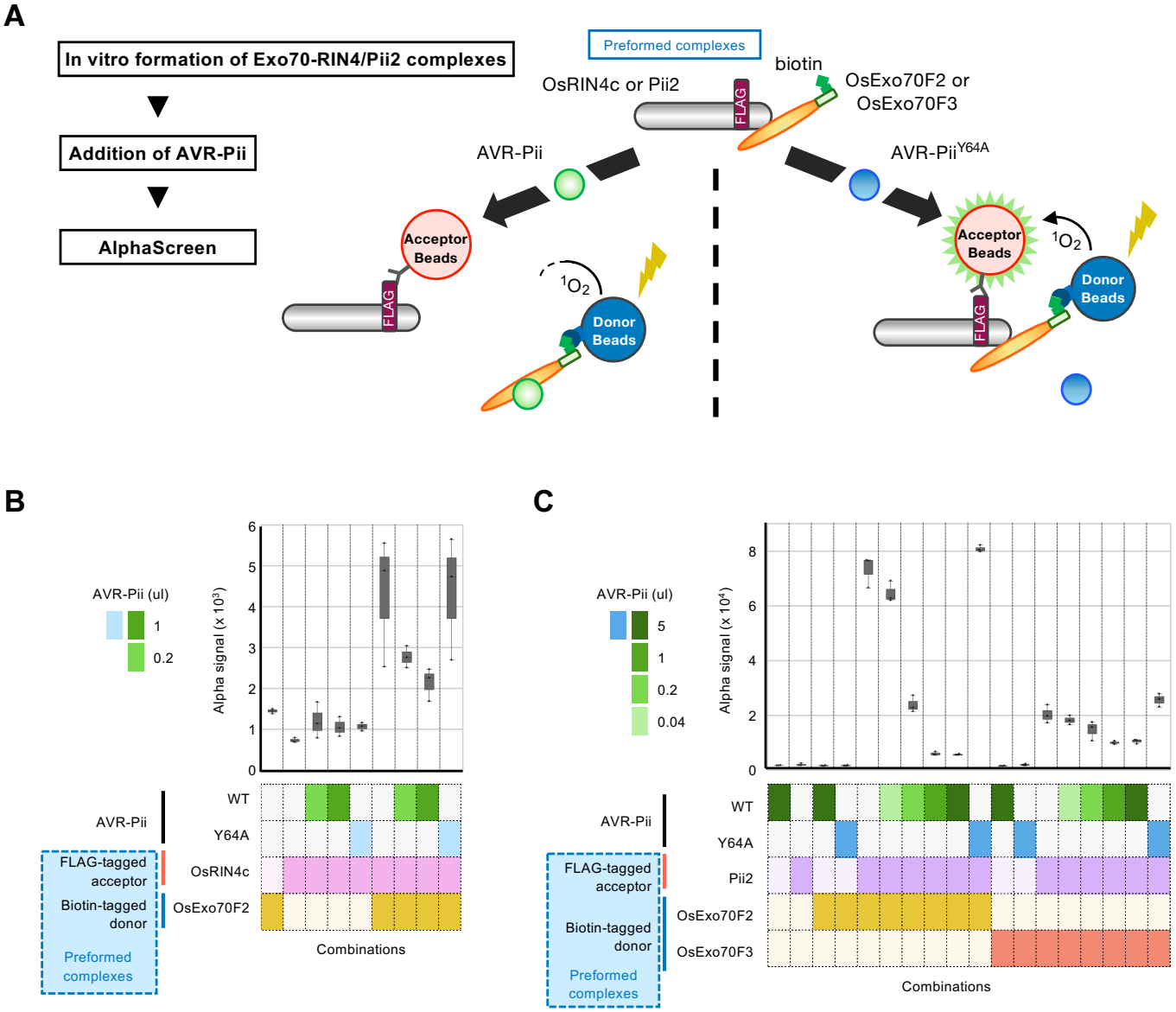
A
In vitro formation of Exo70-RIN4/Pii2 complexes
Addition of AVR-Pii
AlphaScreen
Preformed complexes
OsRIN4c or Pii2
biotin
OsExo70F2 or
OsExo70F3
FLAG
AVR-Pii
AVR-Pii^Y64A
Acceptor Beads
Donor Beads
1O2
B
AVR-Pii (ul)
1
0.2
Alpha signal (x 10^3)
AVR-Pii
WT
Y64A
OsRIN4c
OsExo70F2
FLAG-tagged acceptor
Biotin-tagged donor
Preformed complexes
Combinations
C
AVR-Pii (ul)
5
1
0.2
0.04
Alpha signal (x 10^4)
AVR-Pii
WT
Y64A
Pii2
OsExo70F2
OsExo70F3
FLAG-tagged acceptor
Biotin-tagged donor
Preformed complexes
Combinations

Figure 5. AVR-Pii dissociates the Pii2–OsExo70F2 and Pii2–OsExo70F3 complexes for *Pii2*-mediated resistance

(A) Scheme of AlphaScreen used to detect the effect of AVR-Pii on the interaction of OsRIN4c with OsExo70F2 and that of Pii2 with OsExo70F2. OsRIN4c and OsExo70F2 form a complex *in vitro*, as does Pii2 with OsExo70F2 (Fig. S6). Dissociation of the OsRIN4c–OsExo70F2 or Pii2–OsExo70F2 complex occurs upon addition of AVR-Pii, increasing the distance between the donor bead (bound to OsRIN4 or Pii2) and acceptor bead (bound to OsExo70F2) and thus decreasing the emitted AlphaScreen signals. As the AVR-Pii^{Y64A} mutant does not bind to OsExo70F2, the Pii2–OsExo70F2 complex remains intact, thus producing high AlphaScreen signals. The same assay was conducted with OsExo70F3 in place of OsExo70F2. (B) Effects of AVR-Pii on the preformed OsRIN4c–OsExo70F2 complex. FLAG-tagged OsRIN4c (FLAG-OsRIN4c) and biotinylated OsExo70F2 synthesized via a wheat germ extract (WGE) system were mixed to form the FLAG-OsRIN4c–OsExo70F2 complex (preformed complex), after which the indicated amount of AVR-Pii or AVR-Pii^{Y64A} produced from a WGE system was added to the mixture. After 1 h incubation at room temperature, the FLAG-OsRIN4c–OsExo70F2 interaction was detected by AlphaScreen. WGE without mRNA was used as negative control (indicated as clear rectangles). (C) Effects of AVR-Pii on the preformed Pii2–OsExo70F2 and Pii2–OsExo70F3 complexes. The indicated amount of AVR-Pii or AVR-Pii^{Y64A} produced from a WGE system was added to the preformed complex of Pii2FL2 and biotinylated OsExo70F2 or OsExo70F3, and the OsExo70F2–Pii2FL2 and OsExo70F3–Pii2FL2 interactions were detected by AlphaScreen as described above.

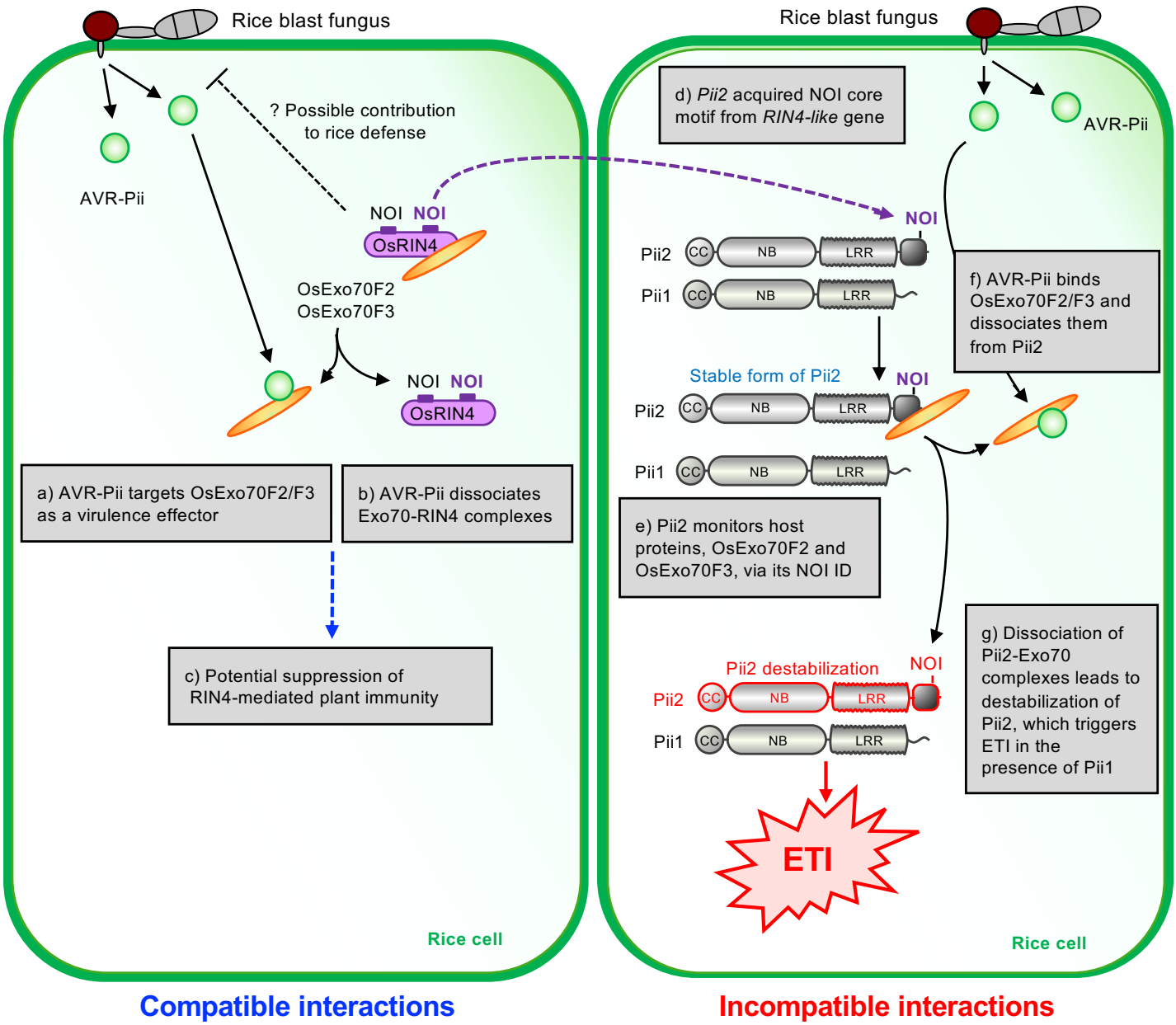

Fig. 6 A possible model of Pii functions.
In the compatible interaction between rice and *M. oryzae* (left panel), the fungal effector AVR-Pii is translocated to the cytoplasm of host cells during infection [Sharma et al., 2013]; and a) AVR-Pii binds host OsExo70F2 and OsExo70F3 [Fujisaki et al., 2015] tethered to OsRIN4-like proteins (which may potentially contribute to rice defense); b) the interactions between AVR-Pii and OsExo70F2/F3 results in dissociation of OsRIN4 from OsExo70F2/F3; c) this may lead to possible suppression of plant immunity; however, this should be confirmed in future study. In the incompatible interaction between rice and *M. oryzae* involving Pii (right panel); d) Pii2 evolutionarily acquired an NOI core motif (PxFGxW) as an integrated domain (ID) from the C-terminal PxFGxW motif of rice RIN4-like proteins; e) Pii2 binds OsExo70F2 and OsExo70F3 via its NOI core motif in the ID, which stabilizes Pii2; f) AVR-Pii binding to OsExo70F2/F3 leads to dissociation of OsExo70F2/F3 from Pii2; g) Dissociation of OsExo70F2/F3 from Pii2 destabilizes Pii2, resulting in the activation of effector-triggered immunity (ETI). The activation of immune responses may be cooperatively executed by Pii1 and Pii2 (Takagi et al., 2017) .

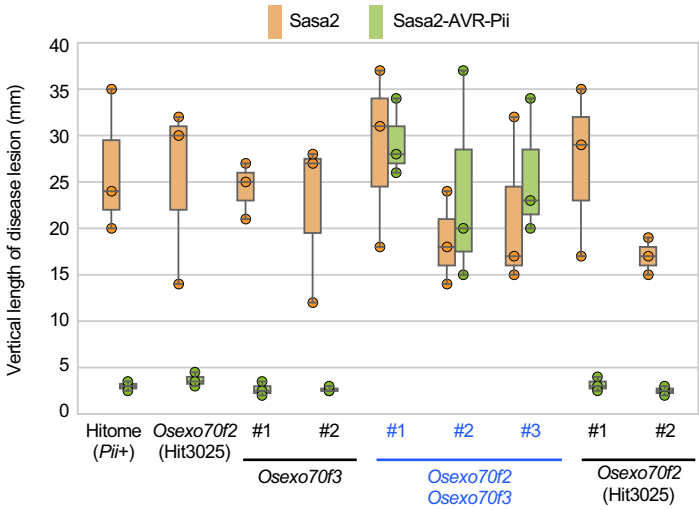

Figure S1. Quantified disease lesion length in rice lines with loss of OsExo70F2 and/or OsExo70F3 function after inoculation with *Magnaporthe oryzae* isolate Sasa2 or Sasa2-AVR-Pii.
Rice blast fungus isolate Sasa2 (without *AVR-Pii*) and transgenic strain Sasa2–AVR-Pii [Yoshida et al., 2009] were used to inoculate rice plants of the single and double knockout mutant lines *Osexo70f2* and *Osexo70f3* in the Hitomebore background (described in Fig. 1). The vertical lengths of disease lesions were measured at 10 days post inoculation.
Boxplots were illustrated from the values of three inoculated spots per line. In the *Osexo70f2 Osexo70f3* double knockout line (labeled in blue), *Pii*-mediated resistance against Sasa2-AVR-Pii was abrogated.

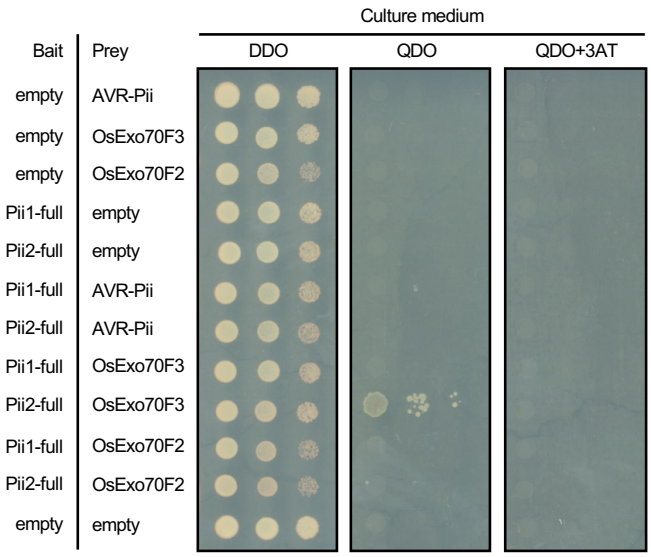

Figure S2. Yeast two-hybrid assay testing the interactions of Pii1 or Pii2 with OsExo70F2, OsExo70F3, or AVR-Pii.

Ten-fold serial dilution of positive yeast transformants were spotted onto double dropout (DDO) medium as control and on quadruple dropout (QDO) medium and QDO medium + 10 mM 3-amino-1,2,4-triazole (3AT) to test interactions. Empty vector (empty) was used as negative control.

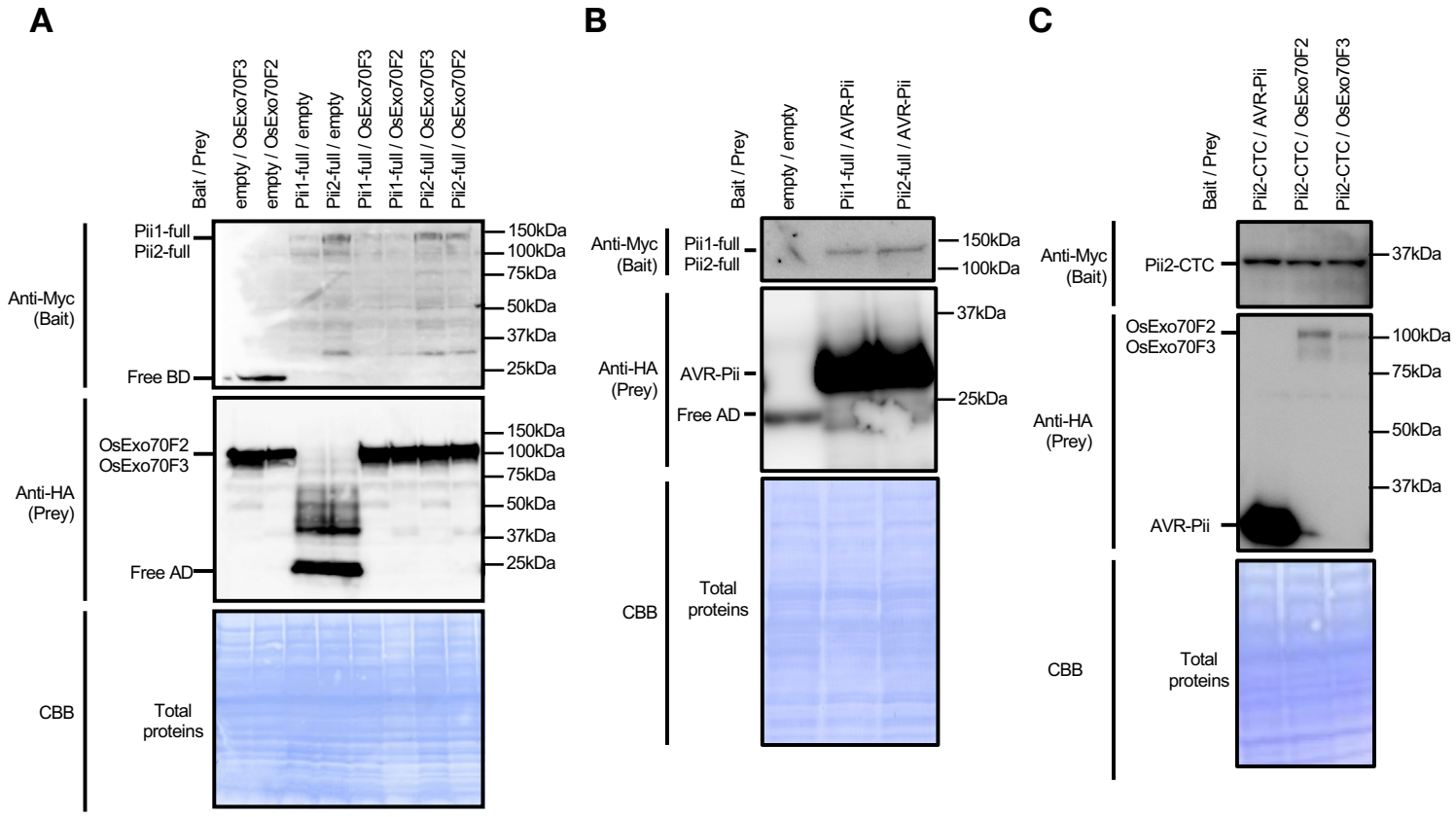

Figure S3. Confirmation of protein production for Pii1, Pii2, AVR-Pii, OsExo70F2, and OsExo70F3 in yeast two-hybrid assays.

(A) Immunoblot analysis showing the accumulation of proteins with the expected molecular weight in yeast cells used in the yeast two-hybrid (Y2H) assays testing the interaction between full-length Pii1 or Pii2 and OsExo70F2 or OsExo70F3 (Fig. S2). The presence of proteins encoded by the bait and prey vectors was probed using anti-Myc and anti-HA antibodies, respectively, as shown in the upper (bait) and lower panels (prey). The expected position of proteins is indicated at left. A Coomassie brilliant blue (CBB)-stained proteins are shown below as loading control. (B) Immunoblot analysis showing the accumulation of proteins with the expected molecular weight in yeast cells used in the Y2H assay testing the interaction between AVR-Pii and full-length Pii1 or Pii2 (Fig. S2). (C) Immunoblot analysis showing the accumulation of proteins with the expected molecular weight in yeast cells used in the Y2H assay testing the interaction between AVR-Pii, OsExo70F2, OsExo70F3, and Pii-2-CTC (Fig. 2B).

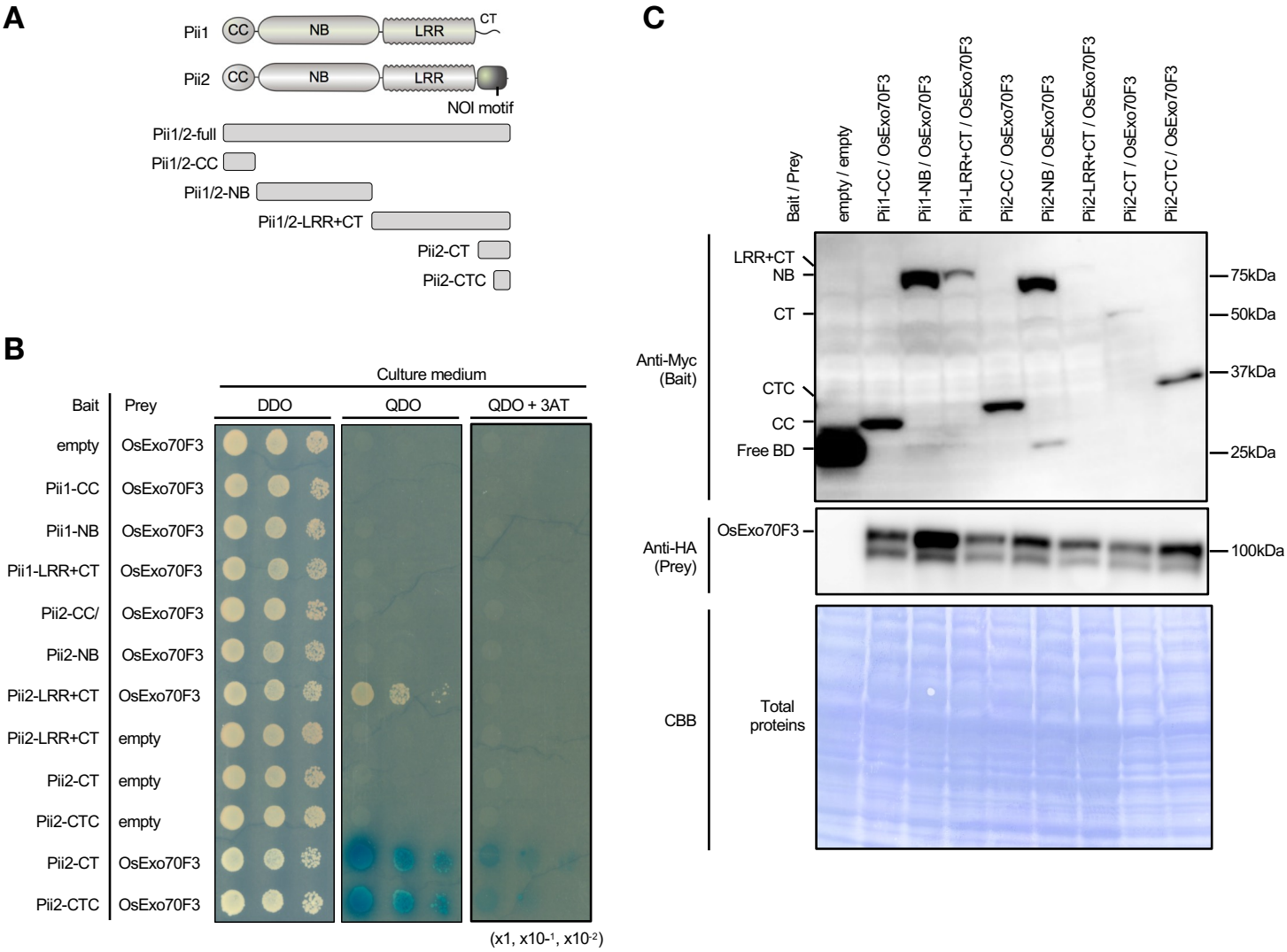

Figure S4. Mapping of the OsExo70F3-interacting regions of Pii2.
(A) Diagram of the functional domains in Pii1 and Pii2 and their truncated variants used for mapping the OsExo70F3-interacting domain. (B) Y2H assay testing the interaction of OsExo70F3 with different regions of Pii1 and Pii2. Ten-fold serial dilution of positive yeast transformants were spotted onto DDO medium as control and on QDO medium and QDO medium + 10 mM 3AT to test interactions. Empty vector (empty) was used as negative control. Bait and prey combinations are listed at left. (C) Immunoblot analysis showing the accumulation of proteins with the expected molecular weight for Pii truncations and OsExo70F3 in yeast cells used in the Y2H assay. The presence of proteins encoded by the bait and prey vectors was probed using anti-Myc and anti-HA antibodies, respectively, as shown in the upper (bait) and lower panels (prey). The expected position of proteins is indicated on the left. A CBB-stained proteins are shown below as loading control.

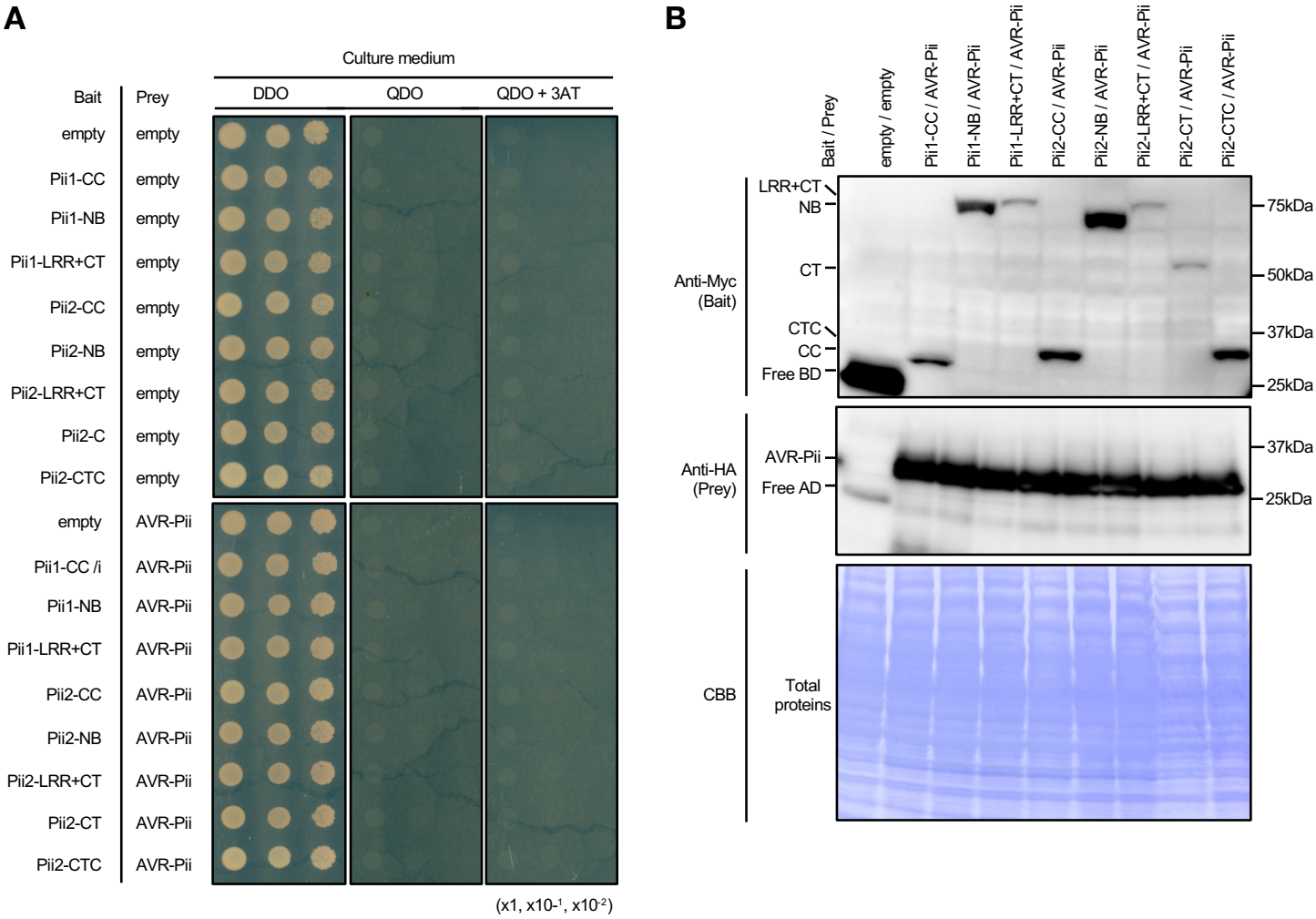

Figure S5. Interactions of AVR-Pii with Pii1 and Pii2 sub-fragments.
(A) Y2H assay addressing the interactions of AVR-Pii with different regions of Pii1 and Pii2. Pii1 and Pii2 sub-fragments used in the assay are indicated in Fig. S4A. Ten-fold serial dilution of positive yeast transformants were spotted onto DDO medium as control and on QDO medium and QDO medium + 10 mM 3AT to test interactions. Empty vector (empty) was used as negative control. Bait and prey combinations are listed at left. (B) Immunoblot analysis showing the accumulation of proteins with the expected molecular weight for Pii truncations and AVR-Pii in yeast cells used in Y2H assay. The presence of proteins encoded by the bait and prey vectors was probed using anti-Myc and anti-HA antibodies, respectively, as shown in the upper (bait) and lower panels (prey). The expected position of proteins is indicated at left. A CBB-stained proteins are shown as loading control.

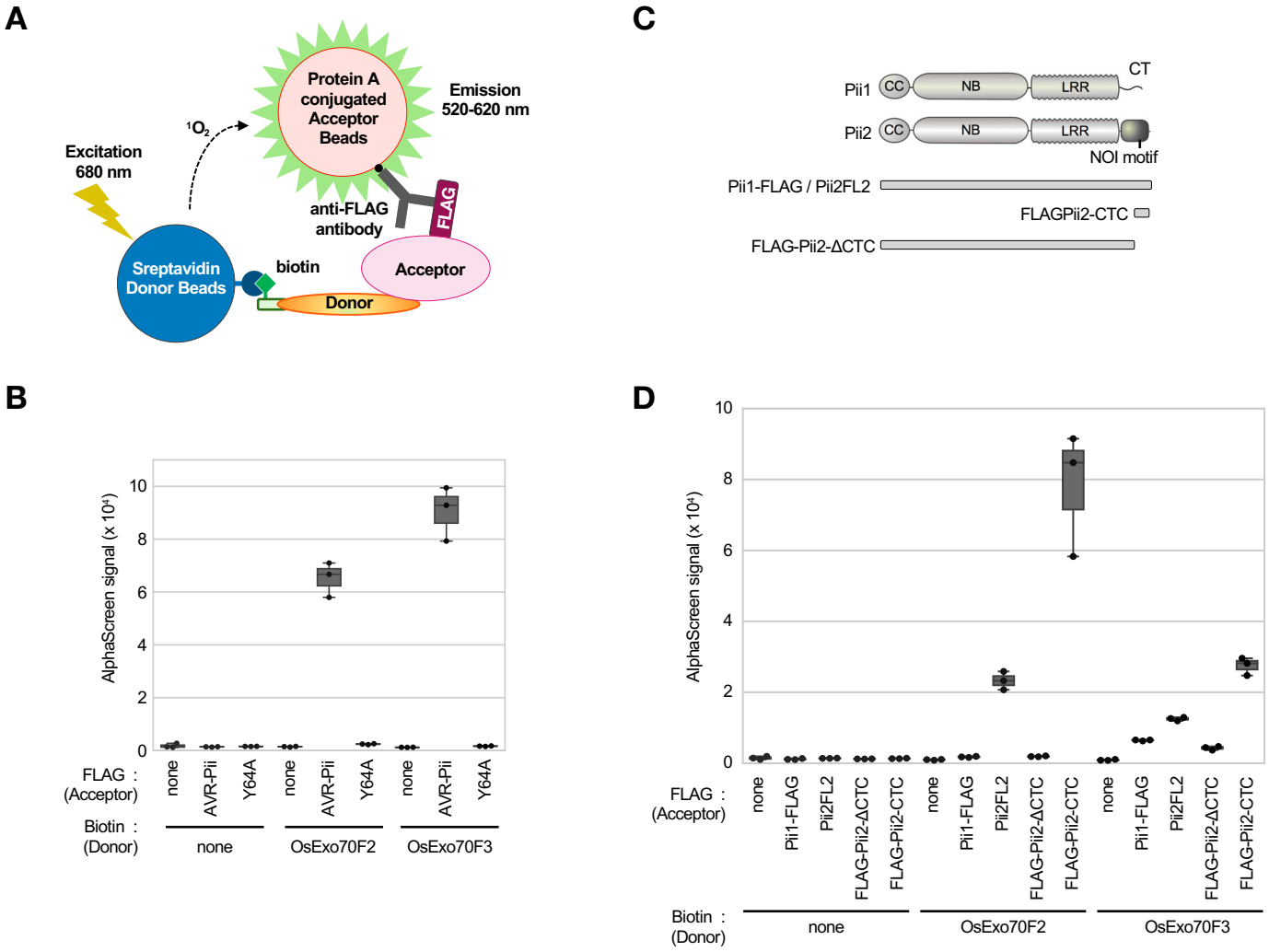

Figure S6. AlphaScreen to investigate the interactions of the components of the Pii system (Pii1, Pii2, OsExo70F2/F3, and AVR-Pii).

(A) Principle of AlphaScreen. Donor beads are excited by illumination at 680 nm, leading to the conversion of ambient oxygen to singlet oxygen ($^1O_2$). Biotinylated proteins bind to streptavidin coating the donor beads, and protein A-conjugated acceptor beads bind to FLAG-tagged proteins via an anti-FLAG antibody. When biotinylated proteins and FLAG-tagged proteins form a complex, they bring the donor and acceptor beads in close proximity, allowing the singlet oxygen to be transferred to the acceptor beads, which become activated and emit fluorescence at 520–620 nm. (B) Interaction tests between biotinylated OsExo70F2 or OsExo70F3 and FLAG-tagged AVR-Pii by AlphaScreen. The AVR-Pii^{Y64A} mutant (Y64A), which does not interact with OsExo70F3 in a Y2H assay nor induces *Pii*-mediated resistance (Fig. S7), was used as negative control. WGE without mRNA added (none) was also used as negative control. Boxplots were illustrated from the values of three technical replicates. (C) Diagrams of full-length Pii1 and Pii2 showing their functional domains and the fragments used for AlphaScreen. (D) AlphaScreen to test the interaction between biotinylated OsExo70F2 or OsExo70F3 and FLAG-tagged full-length Pii1, Pii2, or Pii2 fragments (CTC and ΔCTC). All biotinylated and FLAG-tagged proteins were synthesized in wheat germ extracts (WGE) (Fig. S8), and the indicated WGE products were mixed in the indicated combinations for AlphaScreen. WGE without mRNA added (none) was used as negative control. Boxplots were illustrated from the values of three technical replicates.

Fig. S7

A

AVR-Pii-ns

```
WT AVR-Pii-ns:      MQLSKITFAIALYAIGIAALPTPASLNGNTEVATISDVKLEARSDTTYHKCSKCGYGSDDSDAYFNHKCN
AVR-Piim9-9-ns:     MQLSKITFAIALYAIGIAALPTPASLNGNTEVATISDVKLEASSDTTYHKCSKCGYGSDDSDADFNHKCN
AVR-PiiY64D-ns:     MQLSKITFAIALYAIGIAALPTPASLNGNTEVATISDVKLEARSDTTYHKCSKCGYGSDDSDADFNHKCN
AVR-PiiY64A-ns:     MQLSKITFAIALYAIGIAALPTPASLNGNTEVATISDVKLEARSDTTYHKCSKCGYGSDDSDAAFNHKCN
```

B

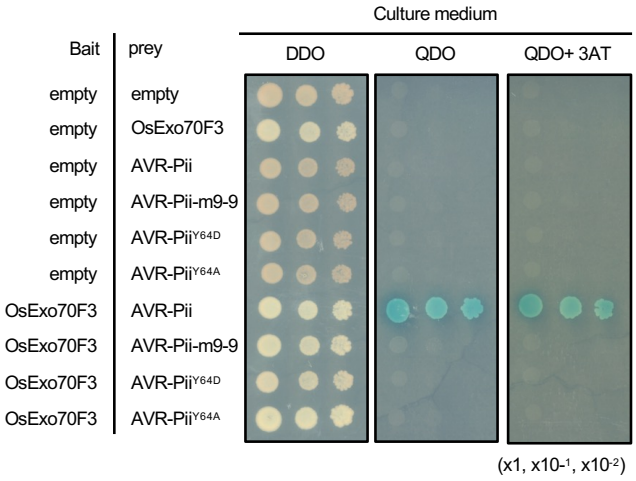

C

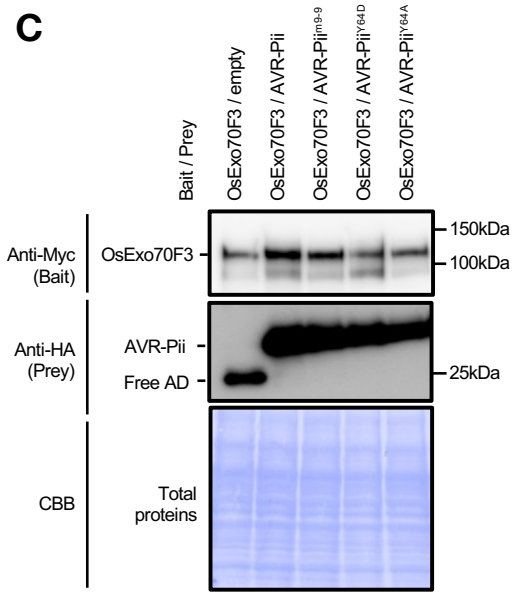

D

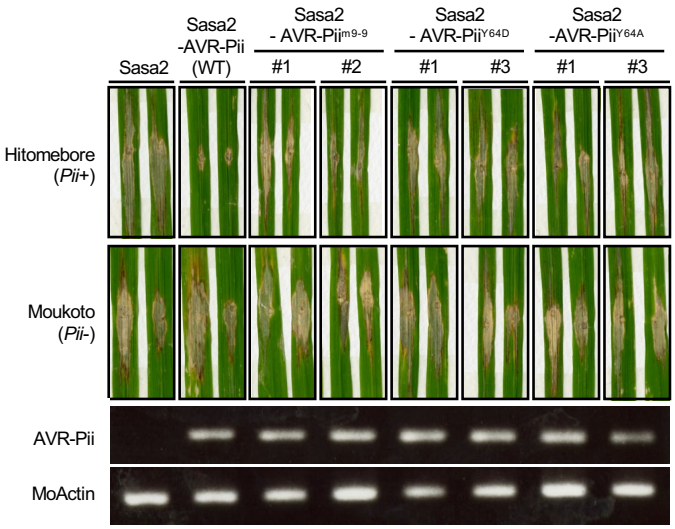

E

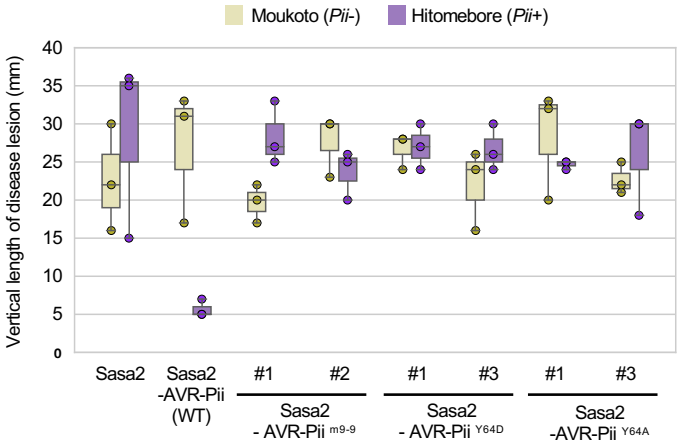

Figure S7. The AVR-Pii mutant AVR-Pii^{Y64A} does not bind OsExo70F3 and is not recognized by Pii. (A) Deduced amino acid sequence of mature AVR-Pii without signal peptide (AVR-Pii-ns) and related point mutants. The sequence of wild-type (WT) AVR-Pii-ns is given in the top row. Arrow head indicate the position of Tyrosine 64. The positions of mutations (m9-9, Y64D and Y64A) in AVR-Pii-ns are marked in red. The mutations were introduced with a Diversify^{TM} PCR random mutagenesis kit (Clontech); the resulting AVR-Pii mutants were used in the Y2H assay below. (B) Y2H assay showing the interaction between OsExo70F3 and wild-type AVR-Pii-ns, but not the AVR-Pii-ns mutants. Ten-fold serial dilution of positive yeast transformants were spotted onto DDO medium as control and on QDO medium and QDO medium + 10 mM 3AT to test interactions. Empty vector (empty) was used as negative control. Bait and prey combinations are indicated at left. (C) Immunoblot analysis showing the accumulation of proteins with the expected molecular weight for OsExo70F3 and wild-type and mutant versions of AVR-Pii-ns in yeast cells used in the Y2H assay. The presence of proteins encoded by the bait and prey vectors was probed using anti-Myc and anti-HA antibodies, respectively, as shown in the upper (bait) and lower panels (prey). The expected position of proteins is indicated on the left. A CBB-stained proteins are shown below as loading control. (D) AVR-Pii mutants (m9-9, Y64D, and Y64A) fail to induce Pii-mediated resistance. *M. oryzae* isolate Sasa2 (without *AVR-Pii*) and the transgenic strain Sasa2 expressing wild-type *AVR-Pii* (Sasa2–AVR-Pii; Yoshida et al., 2009) or AVR-Pii mutants (m9-9, Y64D and Y64A) were spot inoculated onto the rice leaves of the Moukoto (*Pii*−) and Hitomebore (*Pii*+) cultivars. Representative data of disease lesions at 10 days post inoculation are shown. Expression of *AVR-Pii* and *MoActin* was assessed by RT-PCR (bottom). (E) Boxplots showing disease lesion lengths after inoculation of the rice cultivars Moukoto and Hitomebore with *M. oryzae*, which is illustrated from the values of three inoculated spots per line. We used only AVR-Pii^{Y64A} for further study.

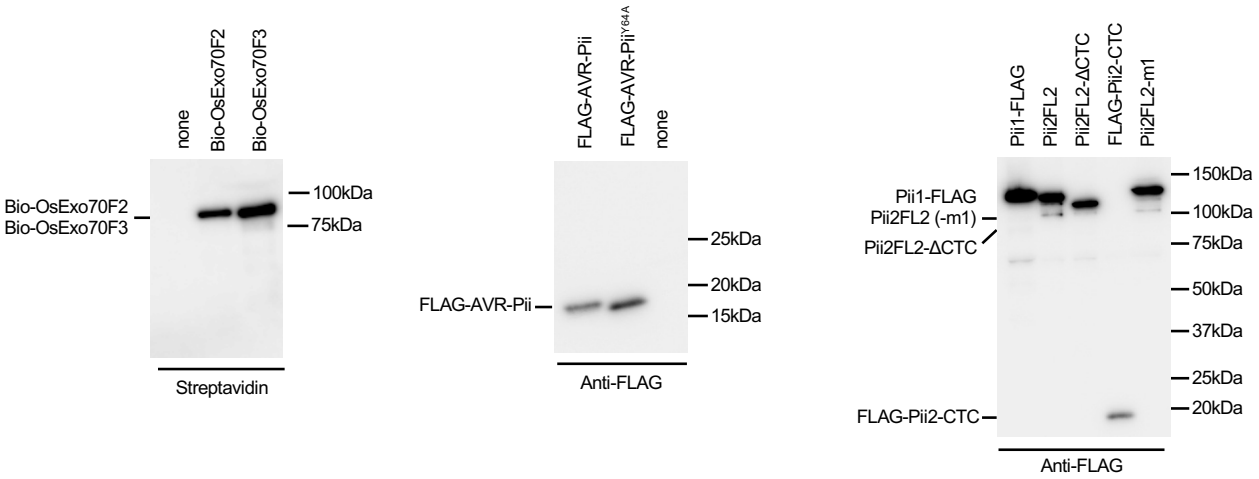

Figure S8. Confirmation of proteins synthesized in the wheat germ translation system used for AlphaScreen.

Biotinylated OsExo70F2 or OsExo70F3 and FLAG-tagged AVR-Pii (FLAG-AVR-Pii), AVR-Pii^{Y64A} (FLAG-AVR-Pii^{Y64A}), Pii1 (Pii1-FLAG), Pii2 (Pii2FL2), and Pii2 derivatives (Pii2FL2-ΔCTC, FLAG-Pii2-CTC and Pii2FL2-m1) were used for AlphaScreen in this study. Biotinylated (left) and FLAG-tagged (middle and right) proteins were detected using streptavidin and anti-FLAG antibodies, respectively.

Fig. S9

A

Pii2

```
1-      MATAGAAVDRLLRRLASGAGHLELPSSIDEDMAHVKRTLARLQDVLLTVEGKYFKMGAEV
                                                 coiled coil
61-     QEWMRKIKQIAYGIQDLLDEFEDSSGTGSQRNGSRISEGTLSCSSAPFFCHLSRSQRIRV

121-    LKRKLDQSTKDTSVFSLLQHSLSNLDKSNEQEVLFHRTEIIGRDTDKENIKNLLLQNDVD

181-    KLPIIPIVGLAGLGKTAVAKLIFHEQGEGWNFDQRIWVHLDKKLDLNKIANSIISQVNQS
                p-loop
241-    VDTTKNQIQNNLQFKRNCLQEVLCDQSSLIVLDDLFSTEENQIAELKEMLRGTKKGTKII
                                  kinase-2            RNBS-B
301-    VTTSSEISAELIHTVPPYKLGPLSEGDCSTIFCQRAFGDGHENSSLTEIAKQIVKRCEGI
            V371D (Hit5882)                                   GLPL
361-    PAVAYSLGSLVRNKNKEAWLYARDKEIWELPTLFPNGFELLASFSEMYLCMPSALKSCFA

421-    YLSTIPKGTIIDREKLIEQWIALDMVGSKHGTLPAYVQGEMFIQQLLSISFLQVRNKPSA
                RNBS-D                                        FL1
481-    TRIRDTNQSKELRIHNLVHDFAMYVARDDLIILDGGEKASSLRKNIPVFYGVVNNDIGQS
                         MHDV
541-    ALRKGLLSSARAVHFKNCKSEKLLVEAFSVLNHLRVLDLSGCCIVELPDFITNLRHLRYL
                      FL3
601-    DVSYSRILSLSTQLTSLSNLEVLDLSETSLELLPSSIGSFEKLKYLNLQGCDKLVNLPPF

661-    VCDLKRLENLNLSYCYGITMLPPNLWKLHELRILDLSSCTDLQEMPYLFGNLASLENLNM

721-    SKCSKLEQLPESLGDLCYLRSFNLSGCSGLKMLPESLKNLTNLEYINLSNIGESIDFNQI

781-    QQLRHILKKTFFSGDIGGSELQTCEHAADSADSKKEITMDFSANLHGNITLPPKCSTEEK
                                  FL2
841-    SGENSERFLSAAIREDSSSTDVSTYVKPVVPSLIGVLRRPTRLDVPAGAMASQVGLAQMP

901-    SSNNGKAGPHPTMAAAQTPETDQPVHKRVRWDDTIDYSCPPNSKPARSASLVQSTDLSTP

961-    KKSYKKIHSMPVVYSSIPKGSSGGTYLMPAKAIASSYRRYSPQRWEQHIGYQGTDEDELM

1021-   VVPPFGEWDHSPTLRKSDFRYEKVFAKLTEEKMSGQRQKPQQRKPRNERFGAVWHAELLQKR
```

NOI core motif
(PxFGxW : AvrRpt2 cleavage site)

B

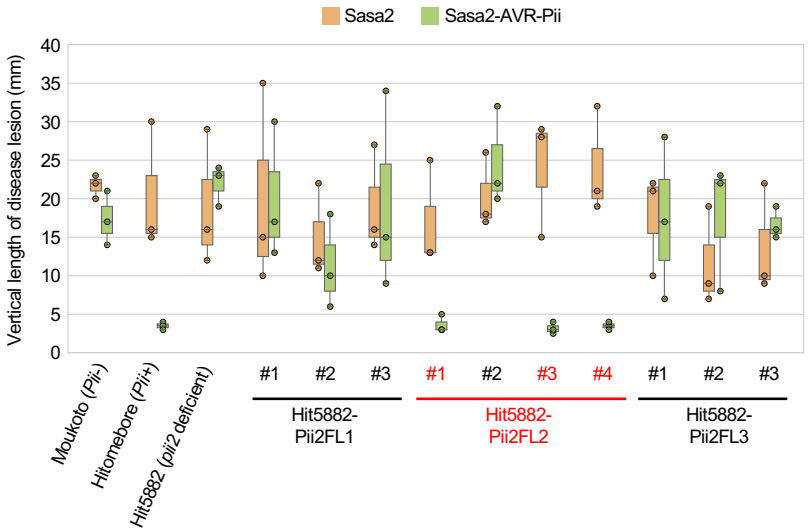

Figure S9. Amino acid sequence and domain structure of Pii2 and the effect of FLAG tag insertions on its AVR-Pii recognition function.

(A) Deduced amino acid sequence of Pii2 from the rice cultivar Hitomebore. The NB and LRR domains are indicated as purple and orange letters, respectively. Coiled coil, P-loop, and other motifs described in Pi5-2 [Lee et al., 2009] are underlined. The NOI core motif (PxFGxW: AvrRpt2 cleavage site) is indicated by green letters. The amino acid residue corresponding to the V371D mutation in a *pii2* mutant (Hit5882) is marked in blue. The Pii2-CT region is indicated in black bold text and Pii2-CTC is indicated by a box. The three insertion sites for the FLAG-tag (FL1, FL2, and FL3) are also shown. (B) Lengths of disease lesions after spot inoculation of rice leaf blades with *M. oryzae* Sasa2 or Sasa2–AVR-Pii. The lesion lengths of Sasa2- and Sasa2–AVR-Pii-inoculated spots in the transgenic rice line Hit5882 expressing FLAG-tagged Pii2 inserted at different positions (*Pii2FL1*, *Pii2FL2*, and *Pii2FL3*) are shown. Boxplots were illustrated from the values of three inoculated spots per line. None of the lines of Hit5882-*Pii2FL1* or Hit5882-*Pii2FL3* showed resistance, whereas three lines of Hit5882-Pii2FL2 showed resistance. Therefore, the *Pii2FL2* construct was used in this study to retain Pii2 function in a FLAG-tagged form.

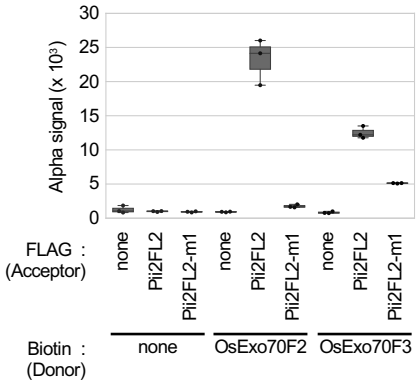

Figure S10. The NOI core motif of Pii2 ID is crucial for its interaction with OsExo70F2 and OsExo70F3.

Interaction test between the Pii2-m1 mutant and OsExo70F2 or OsExo70F3 as studied by AlphaScreen. Boxplots were illustrated from the values of three technical replicates. For the confirmation of proteins used in the assay, see Figure S8.

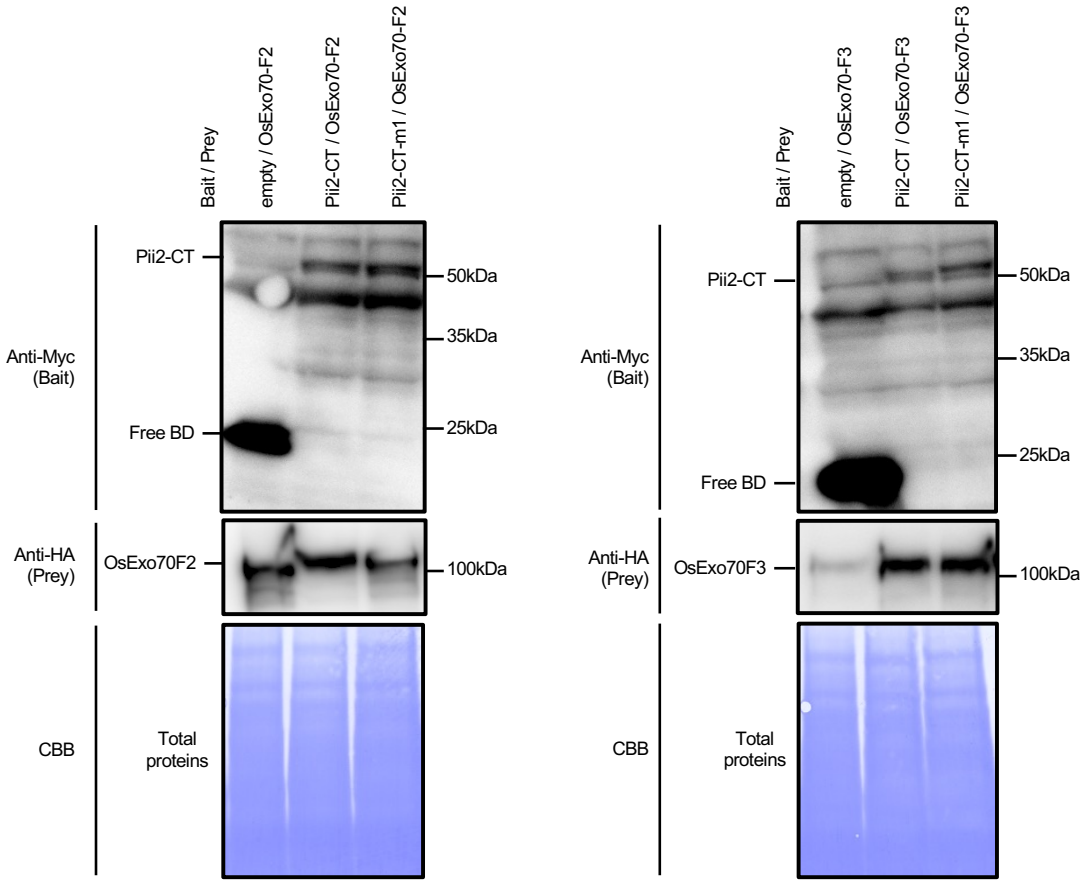

Figure S11. Confirmation of accumulation of OsExo70F2, OsExo70F3, Pii2-CT, and Pii2-CT-m1 proteins in yeast cells used for Y2H.

Immunoblot analysis showing the accumulation of proteins with the expected molecular weight in yeast cells used in the Y2H assay (Fig. S10) testing the interaction between OsExo70F2 and Pii2-CT or Pii2-CT-m1 (left) or between OsExo70F3 and Pii2-CT or Pii2-CT-m1 (right). The presence of proteins encoded by the bait and prey vectors was probed using anti-Myc and anti-HA antibodies, respectively, and shown in the upper (bait) and lower panels (prey). The expected position of proteins is indicated on the left. A CBB-stained proteins are shown below as loading control.

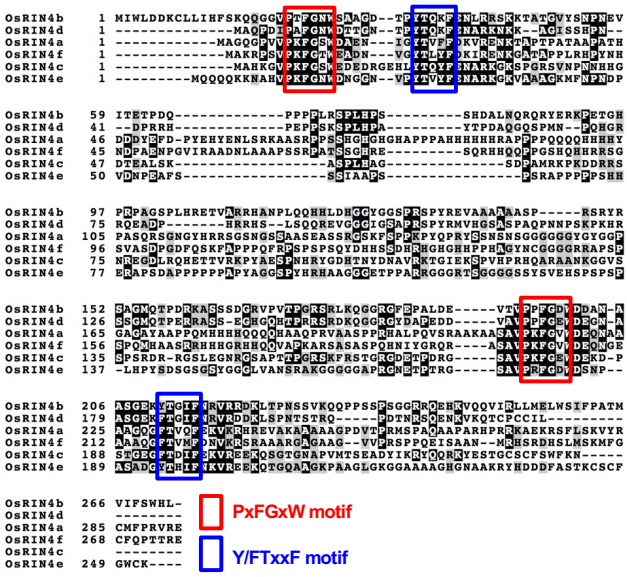

Figure S12. Multiple amino acid sequence alignment of rice RIN4-like proteins.
Rice RIN4-like proteins, OsRIN4a (Os02g0189400), OsRIN4b (Os02g0504700), OsRIN4c (Os03g0848600), OsRIN4d (Os04g0379600), OsRIN4e (Os08g0526400), and OsRIN4f (Os06g0636100) were identified by BLAST search using Arabidopsis RIN4 as query; the alignment was generated using CLUSTALW (https://www.genome.jp/tools-bin/clustalw). Two conserved motifs (PxFGxW and Y/FTxxF) in RIN4-like proteins are indicated by the red and blue open boxes, respectively.

OsNOIa (Os04g0620600)

MTTMDKGRALPKFGEWDVKNPASAEGFTVIFQKARDDKKTTGPGNARVGIPPAFRSTDDDGGYRPE
FKPAESYQQHTPPKRVKKKWAFCAGC

OsNOIb (Os09g0253000)

MAAEKGSPLPKFGEWDVNDPASAEGFTVIFNKARDEKKTGGNSQGQDLAAKSEQPSGQGLYPAKP
NSSKKWFCCMQPTAAES

OsNOIc (Os11g0226400)

MSQARSLNFYGLAECLPSTLQFKQLRVLILEFWDDQEEFDLRGIFRLLQLRYVQVTTDMIVKLPATV
QSLQYLETLQLNARVANVPSDIVHLPKLLHLRLRDVANLPDNIGCMASLCTLESLDLSNNSEQNVW
GLGEMTNLQELYLNCSTELSGRLKRNLTALASSLGKLRKLRTLILAPSSGTSMYMDCSSIVSSPPL
CLQRLELLPTICIFSRLPKWIGQLKRLRILKIVVRELLCSDVHSLTMLQELTVLSLDVQQSTEETIVFN
DKAFPVLKYFKFRCGVLRLAFQAEAMPNLRKLKIEFNVHRGEQYGDILTGIEHLLNLQEIIGQIGAAA
GAEESDKRAAEFALSDATKKHSRISRFNIRWINCVEEDVRVSKISDLQGISSSSDEEKQKANEPSGT
DITIEDESPFSHEPNYDVPRAYKAEIESEEVPHAELADASRTSDSIDNRRRQRRSIEPSFSRDRLSQP
RKHSVASAVPKFGEWDSPLRPADNYTSIFNRAREEKRSQVEKPSVFDKDDLLVRRTRNRNDGHA
STKCSCFGWCK

Red : PxFGxW motif

Figure S13. Amino acid sequences of rice PxFGxW motif-containing proteins that are not related to OsRIN4.

Deduced amino acid sequences of rice PxFGxW motif–containing proteins used in this study. A BLAST search using Arabidopsis RIN4 as query identified three PxFGxW motif–containing proteins that are not related to OsRIN4s. These proteins were designated as OsNOIa (Os04g0620600), OsNOIb (Os09g0253000), and OsNOIc (Os11g0226400). The PxFGxW motif is marked in red text.

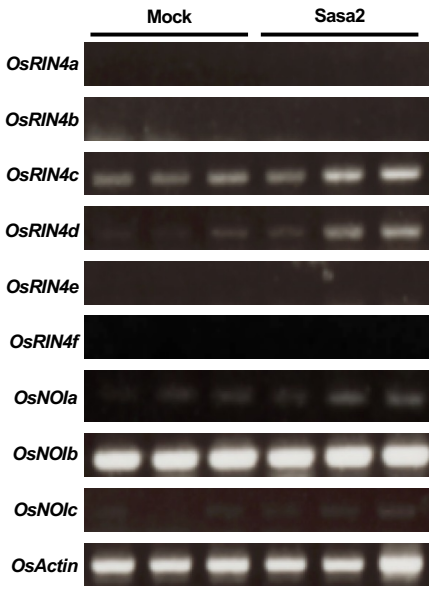

Figure S14. Expression of *RIN4-like* genes and other genes encoding NOI-containing proteins in rice leaves.

RT-PCR analysis was used to confirm the expression of *RIN4-like* genes and other genes encoding NOI-containing proteins in rice leaves. Leaves of the rice cultivar Hitomebore were mock-inoculated or inoculated with rice blast fungus (Sasa2); leaves were harvested at 3 days post-inoculation, and total RNAs were extracted and used for RT-PCR using specific primers. *OsACTIN* served as a positive control.

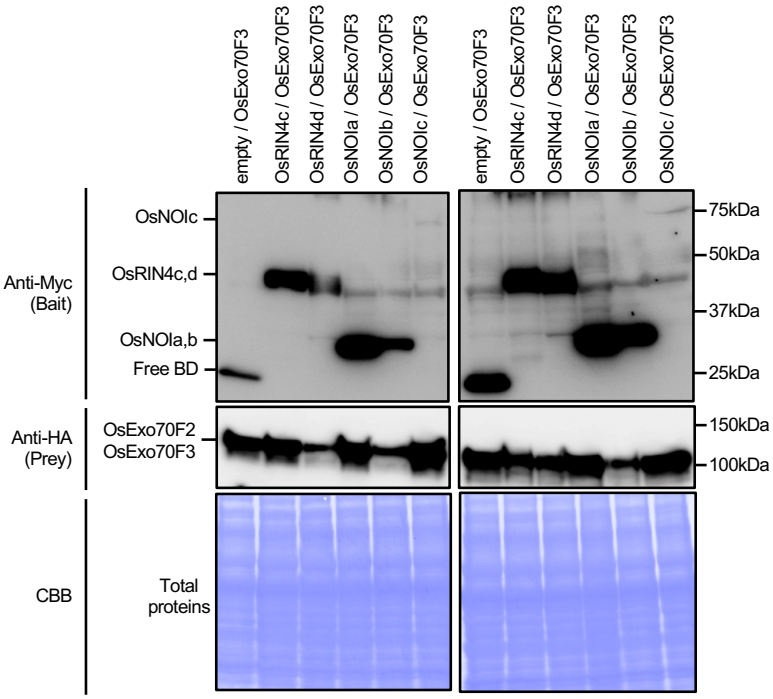

Figure S15. Confirmation of accumulation of OsExo70F2, OsExo70F3, and PxFGxW motif–containing proteins in yeast cells used in the Y2H assay.

Immunoblot analysis showing the accumulation of proteins with the expected molecular weight in yeast cells used in Y2H assay testing the interaction between OsExo70F2 or OsExo70F3 and rice PxFGxW motif–containing proteins (Fig. 1F). The presence of proteins encoded by the bait and prey vectors was probed using anti-Myc and anti-HA antibodies, respectively, and is shown in the upper (bait) and lower panels (prey). The expected position of proteins is indicated at left. A CBB-stained proteins are shown below as loading control.

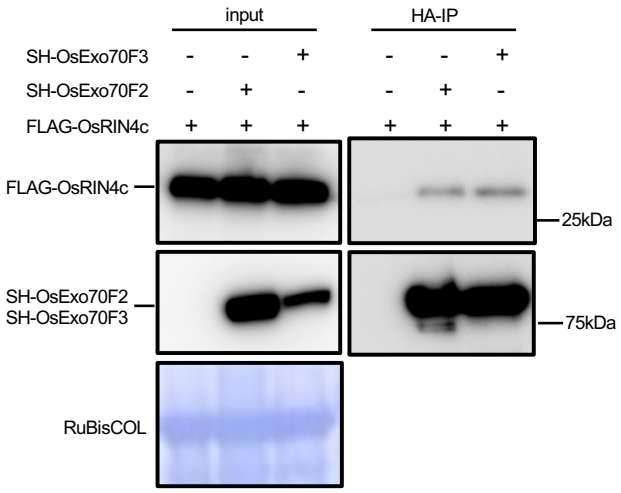

Figure S16. Confirmation of the interaction between OsRIN4c and OsExo70F2 or OsExo70F3 by co-immunoprecipitation assay.

Constructs encoding FLAG-tagged OsRIN4c and/or StrepII-HA (SH)-tagged OsExo70F2/F3 were infiltrated into *N. benthamiana* leaves in the indicated combinations. The infiltrated leaves were sprayed with 30 μM dexamethasone, and total proteins were extracted at 2 days after the treatment for co-immunoprecipitation with anti-HA antibodies. CBB-stained RuBisCOL (Rubisco large subunit) are shown below as loading control of input proteins.

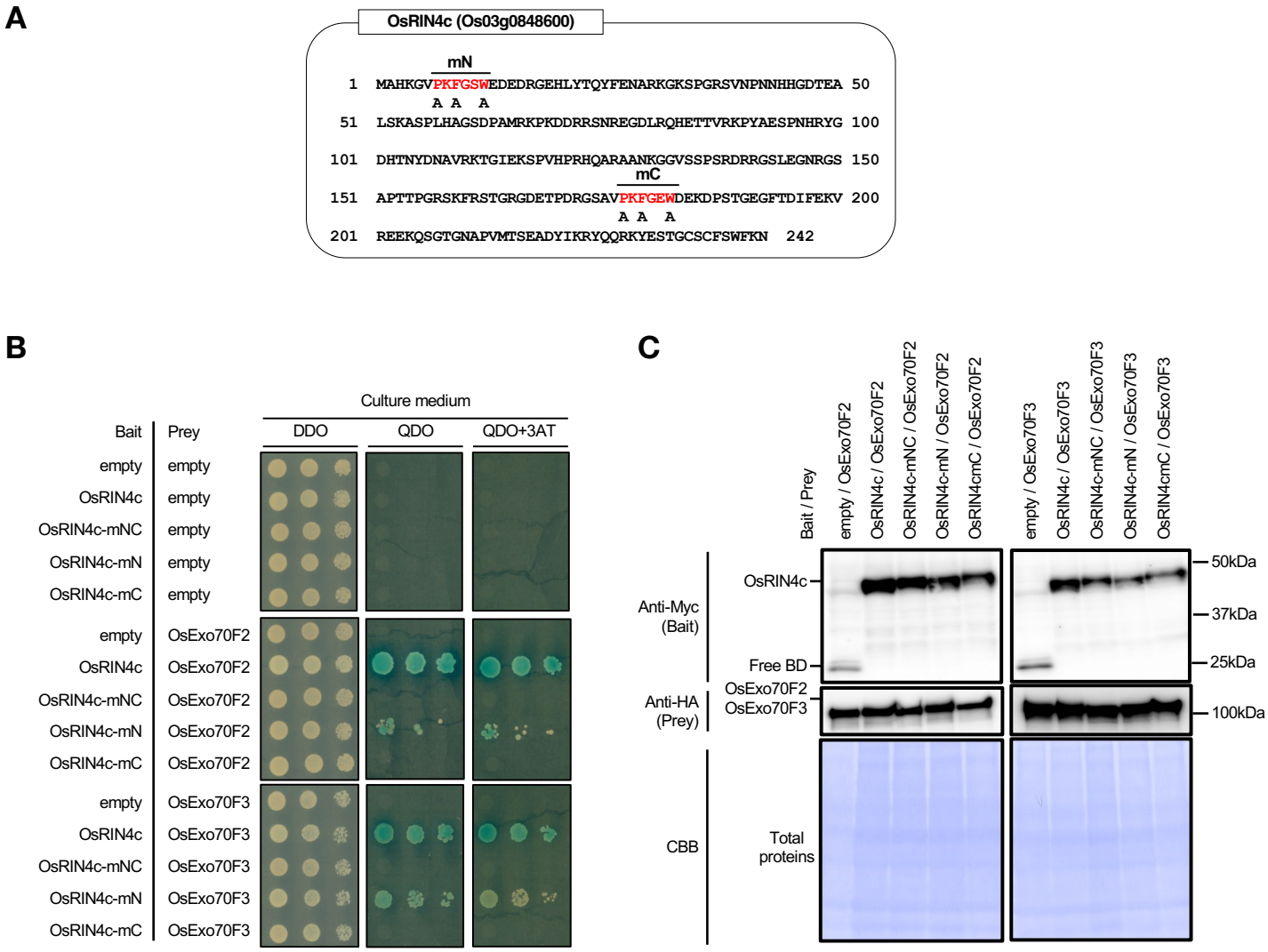

Figure S17. The C-terminal NOI core motif of OsRIN4c is involved in its interaction with OsExo70F2 and OsExo70F3.

(A) Positions of the mutations in the mN and mC variants of the PxFGxW motif (red letters) of OsRIN4c. (B) Y2H assay to test the interaction of OsExo70F2 or OsExo70F3 and intact OsRIN4c or OsRIN4c carrying the mN and/or mC mutations. Ten-fold serial dilution of positive yeast transformants were spotted onto DDO medium as control and on QDO medium and QDO medium + 10 mM 3AT to test interactions. Empty vector (empty) was used as negative control. Bait and prey combinations are listed at left. (C) Immunoblot analysis showing the accumulation of proteins with the expected molecular weight in yeast cells used in the Y2H assay testing the interaction between OsExo70F2 or OsExo70F3 and OsRIN4c. The presence of proteins encoded by the bait and prey vectors was probed using anti-Myc and anti-HA antibodies, respectively, and shown in the upper (bait) and lower panels (prey). The expected position of proteins is indicated at left. A CBB-stained proteins are shown below as loading control.

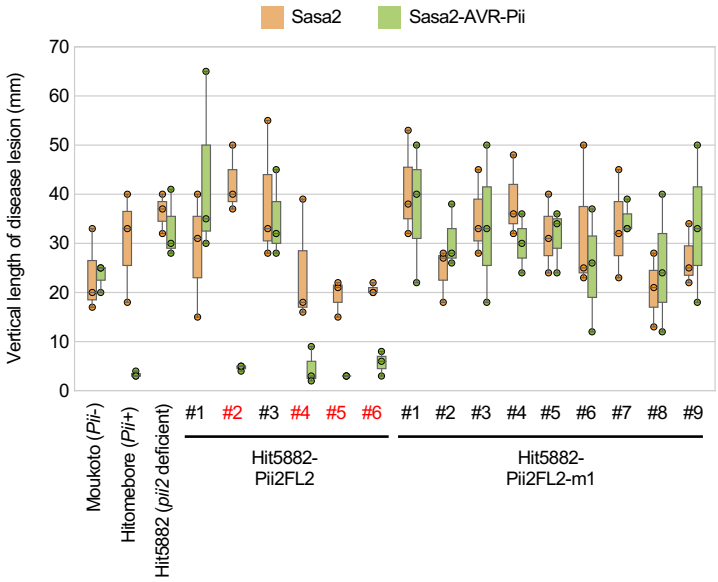

Figure S18. The Pii2 variant carrying the m1 mutation does not induce resistance against AVR-Pii.

Length of disease lesions in the rice lines tested. Boxplots were illustrated from the values of three inoculated spots of rice blast fungus Sasa2 (lacking *AVR-Pii*) and Sasa2–AVR-Pii (with *AVR-Pii*) per line. The ttransgenic lines showing *Pii*-mediated resistance are marked by red letters.

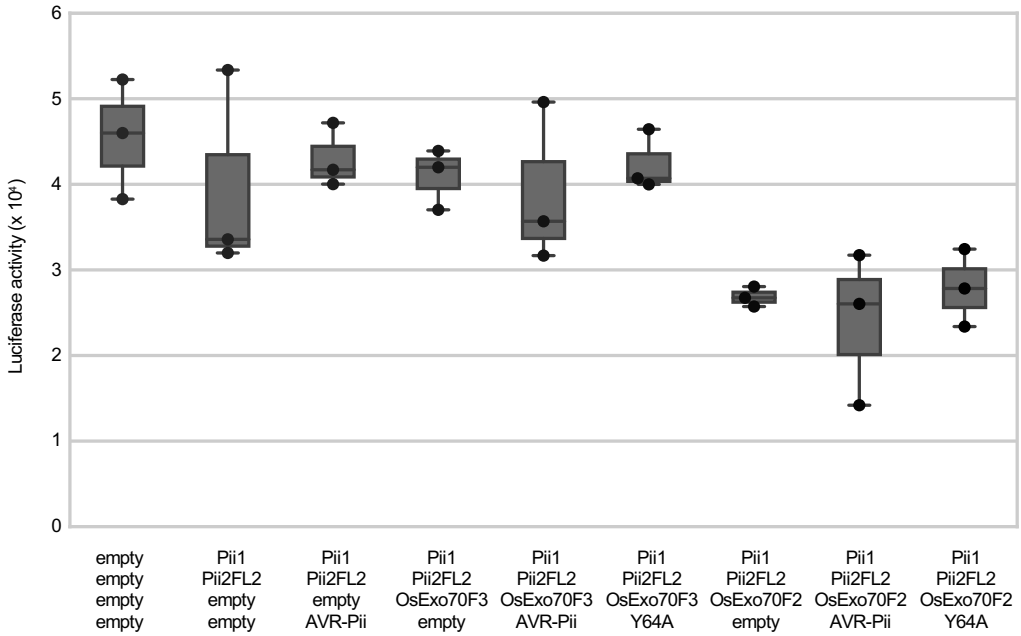

Figure S19. Viability of rice protoplasts transfected with various Pii components.
Cell viability was estimated as described previously (Yoshida et al., 2009). *Firefly luciferase* gene was expressed under the control of Cauliflower mosaic virus 35S promoter in ice protoplasts (Oc cell). Several expression vectors of the components of *Pii*-mediated resistance (Pii1, Pii2FL2, OsExo70F2, OsExo70F3, FLAG-AVR-Pii and FLAG-AVR-Pii^{Y64A}) were also co-expressed. The combinations of expression vectors are indicated bellow. FLAG-AVR-Pii and FLAG-AVR-Pii^{Y64A} are indicated as AVR-Pii and Y64A, respectively. Protoplasts were collected at 20 hours post-transfection, and luciferase activity was measured. Boxplots were illustrated from the values of three technical replicates.

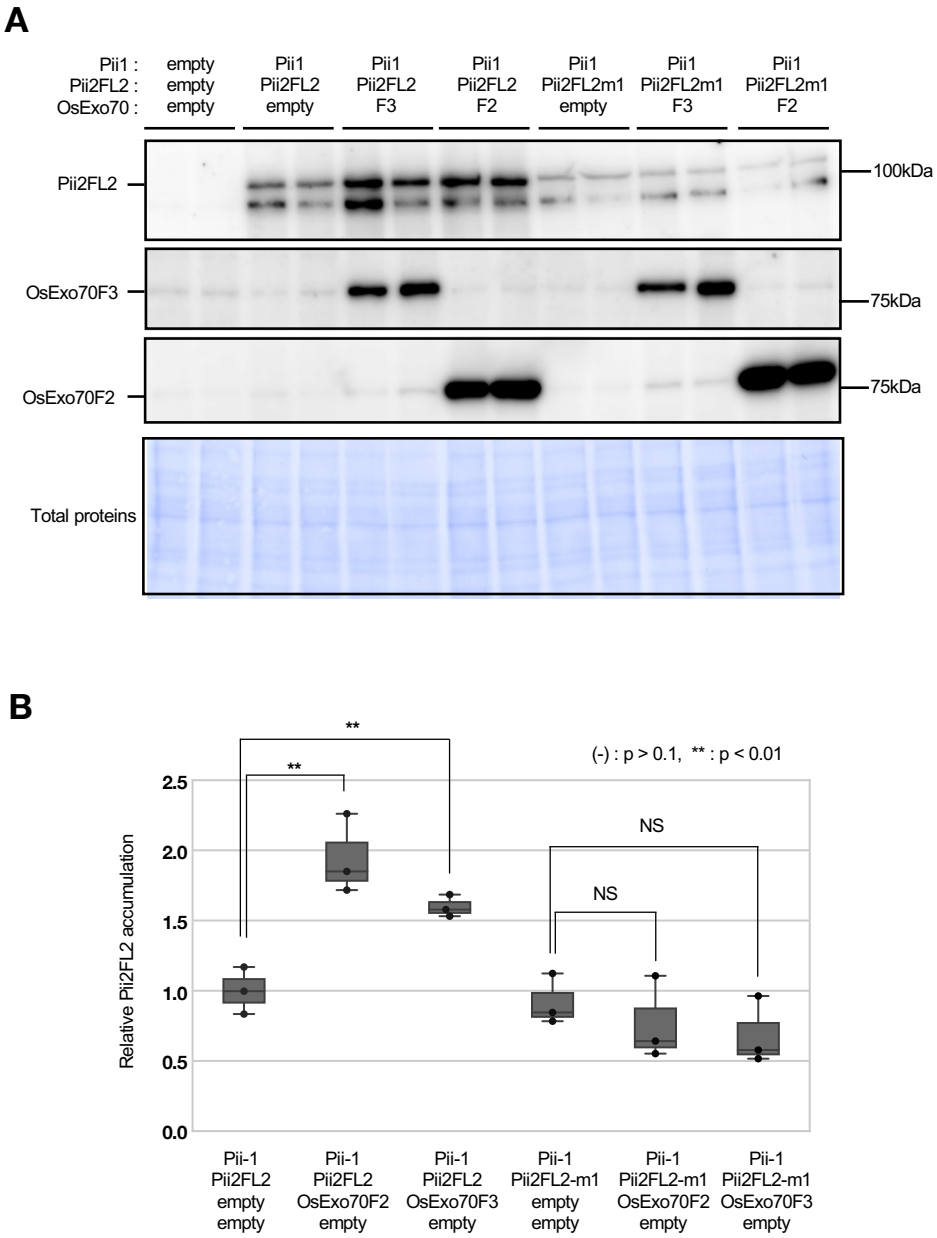

Figure S20. Effects of the m1 mutation on OsExo70F2- or OsExo70F3-mediated stabilization of Pii2FL2 in rice Oc protoplasts.

(A) Representative data for the abundance of Pii2FL2 and Pii2FL2-m1 when their encoding constructs were co-expressed with or without *OsExo70F2* or *OsExo70F3* in rice Oc protoplasts. (B) Quantification of the abundance of Pii2FL2 and Pii2FL2-m1 shown in (A). Protein band intensity was quantified using ImageJ (https://imagej.net/ij/). Double asterisks represent significant differences (*t*-test; $P<0.01$), and NS indicates no significant differences in Pii2FL2 accumulation levels. Boxplots were illustrated from the values of three technical replicates.

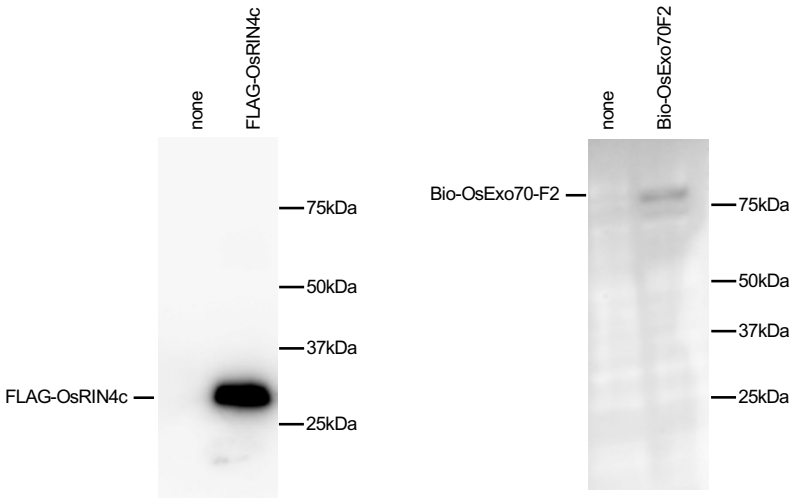

Figure S21. Confirmation of proteins synthesized by WGE used for AlphaScreen.
(A) Biotinylated and FLAG-tagged proteins for AlphaScreen were synthesized in the WGE system. Biotinylated OsExo70F2 and FLAG-tagged OsRIN4c (FLAG-OsRIN4c) were used for the AlphaScreen (Fig. 5B). Biotinylated (right) and FLAG-tagged (left) proteins were detected using streptavidin and anti-FLAG antibodies, respectively.